This project is cofinanced by the European Union.
Ministry of Science, Education and Sports

Sveučilište u Zagrebu
Fakultet elektrotehnike i računarstva

Upravljanje otporno na kvarove generatora i smanjenje vibracija pri upravljanju momentom generatora vjetroagregata

dr.sc. Vinko Lešić

Sadržaj prezentacije

- Kvarovi generatora i motivacija
- Upravljanje otporno na kvarove generatora
- Utjecaj na sustav vjetroagregata
- Smanjenje vibracija pri upravljanju momentom generatora
- Zaključak

Kvarovi generatora i motivacija

Wind energy today

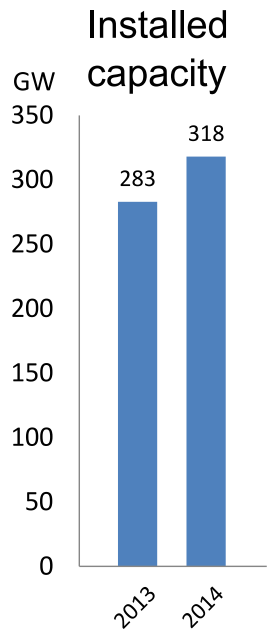

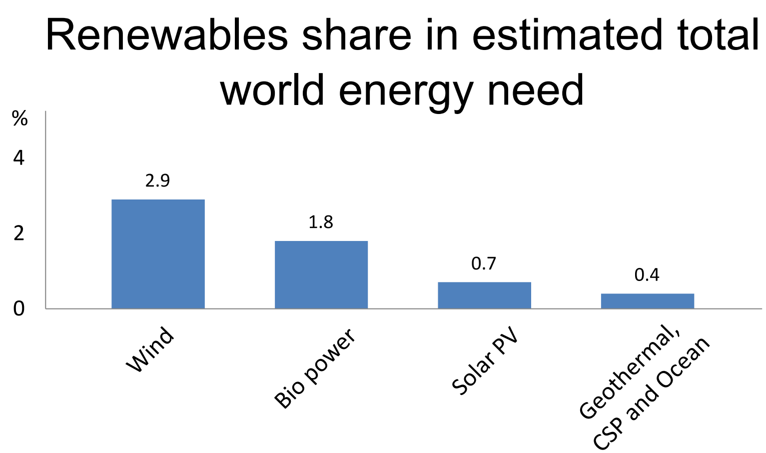

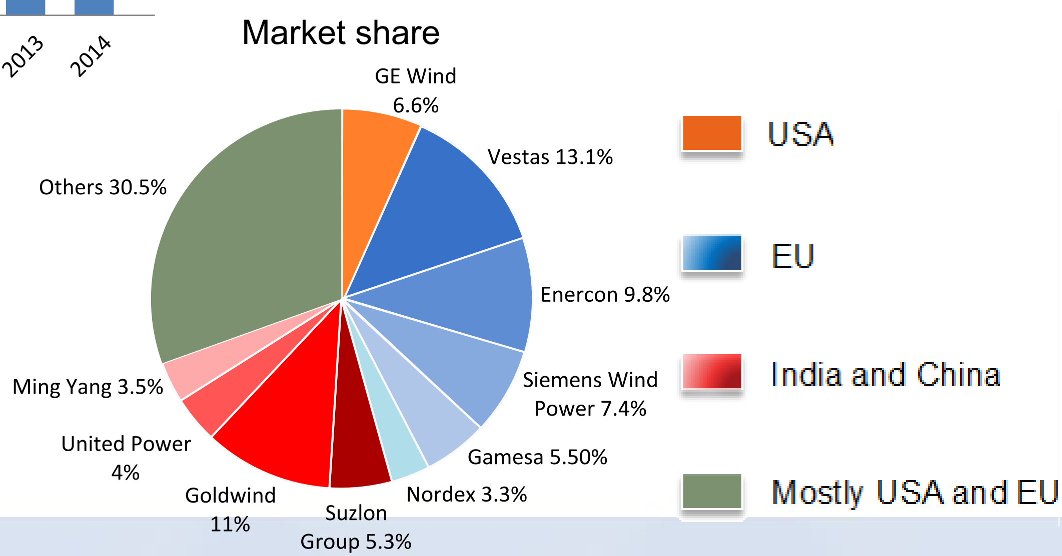

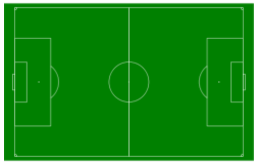

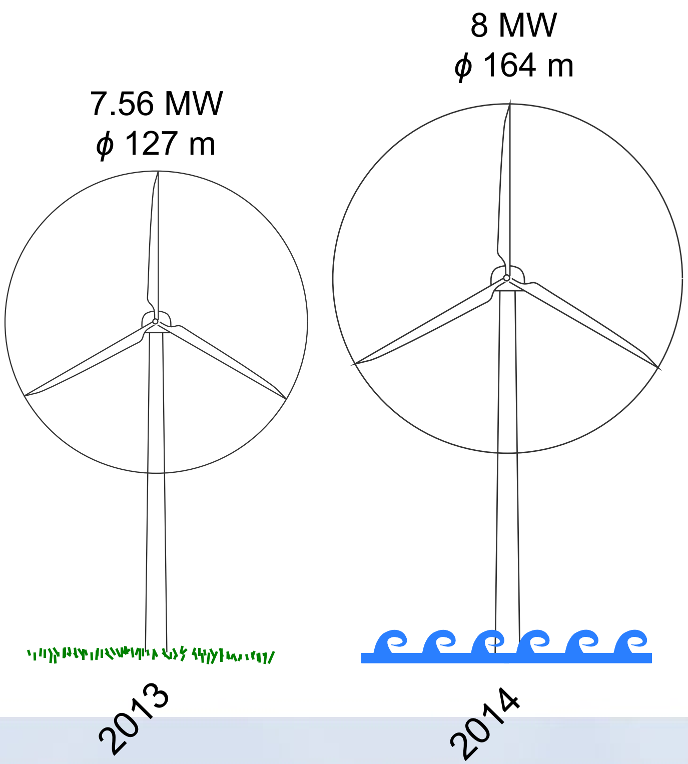

Motivation

Wind turbine faults

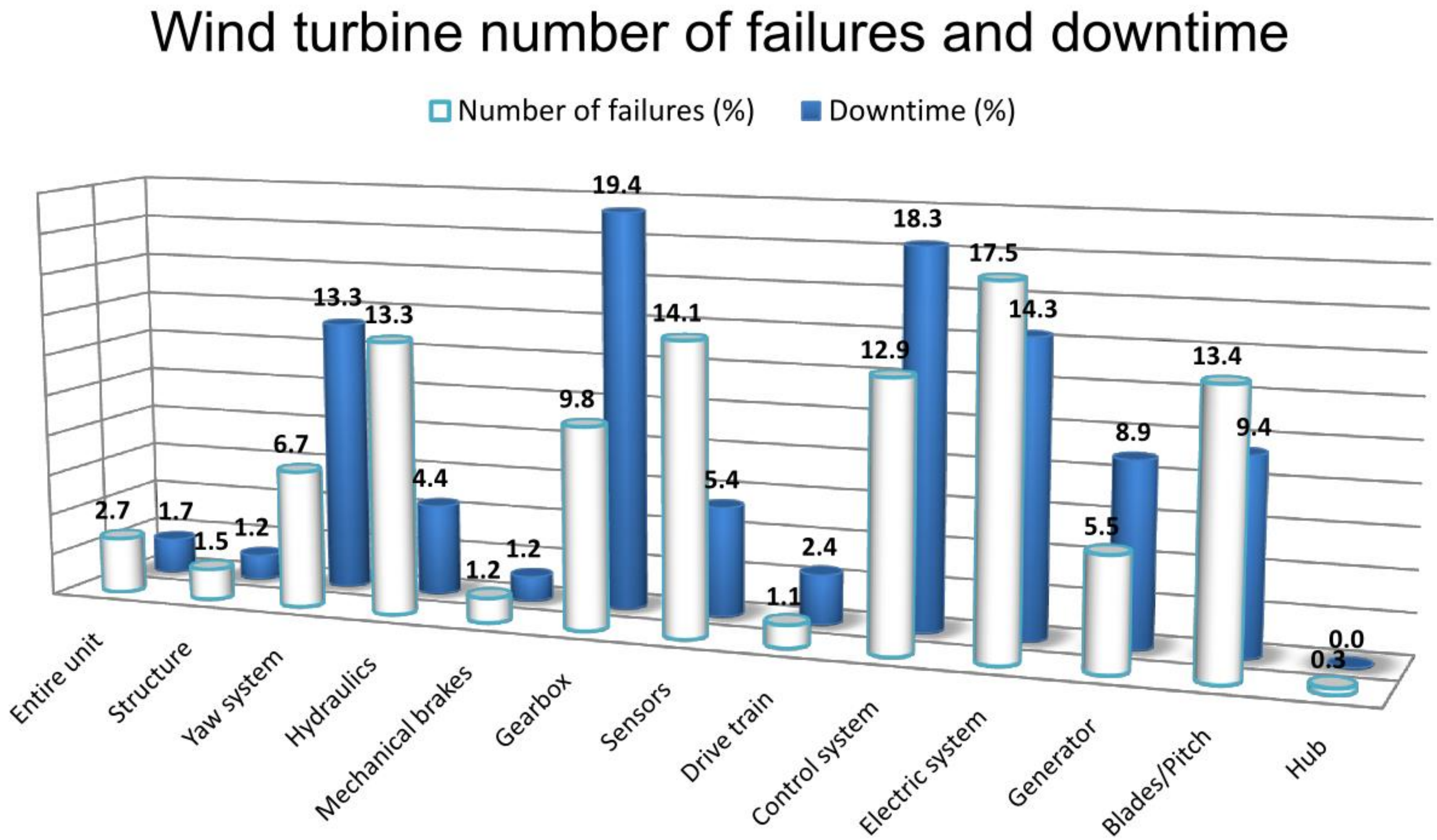

Source: J. Ribrant 2007. (Swedish wind turbines 2000.-2004.)

Wind turbine faults

- Gearbox concept and direct-drive

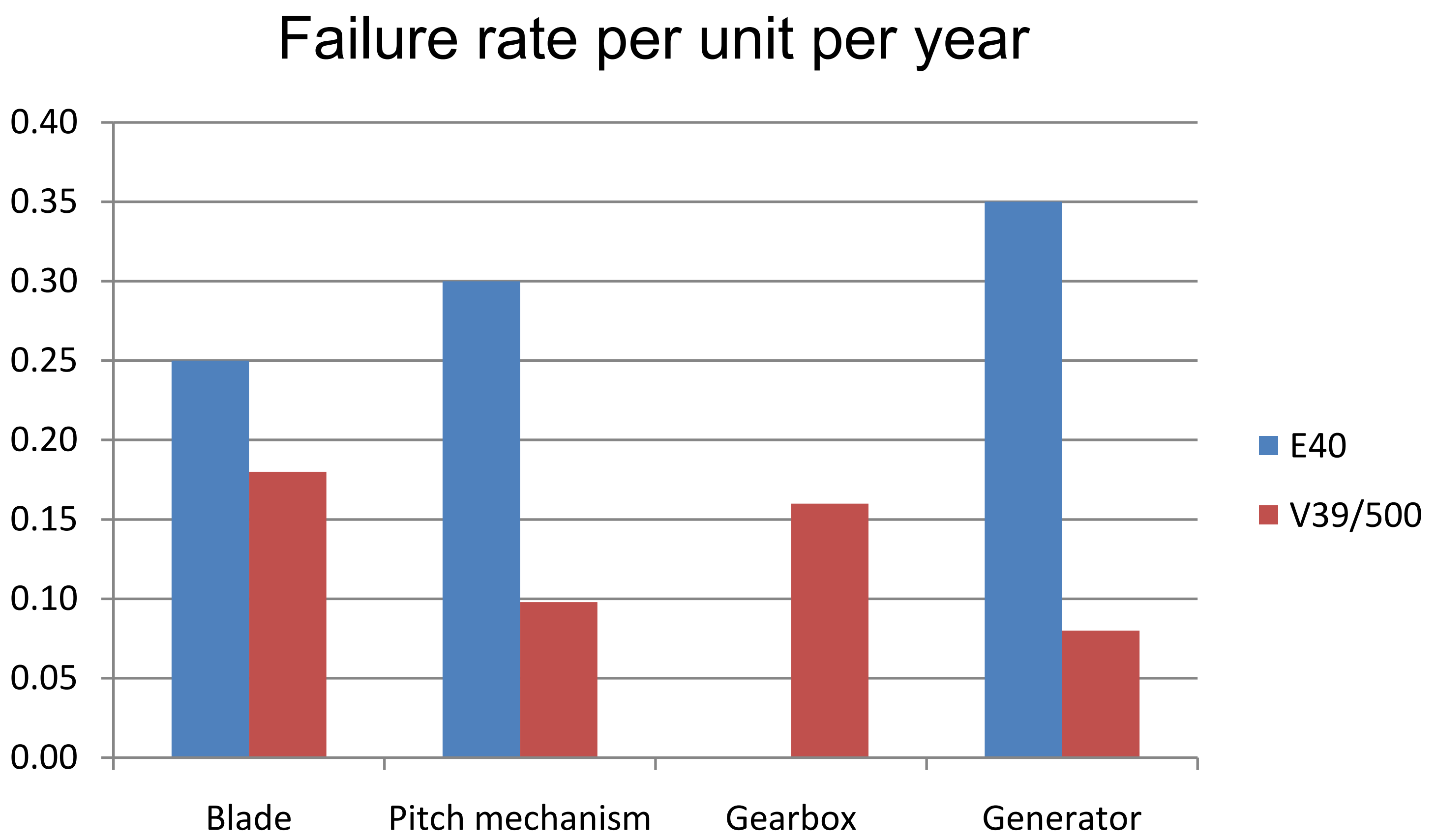

Source: J. Ribrant 2007. (Swedish wind turbines 2000.–2004.)

Generator faults

- Electric machines failure frequency in wind turbines is about **10 times** greater than in industry applications
  - harsh environment
  - frequently varying operating conditions
- In industry applications:
  - 35% of faults – stator related (e.g. insulation degradation)
  - 30% of induction machine faults – rotor related (cage)
- Wind turbines are placed on hardly reachable, remote locations
- Lots of expensive monitoring and control equipment is already installed → great opportunity for diagnostics and control system interventions

Observed faults

- Cage defects (squirrel-cage induction generator)
- Stator insulation faults
- Both kinds of faults can be related with instantaneous rotor flux linkage position

Observed faults

- Cage defects (squirrel-cage induction generator)
- Stator insulation faults
- Both kinds of faults can be related with instantaneous rotor flux linkage position
- Faults spread rapidly in normal operation

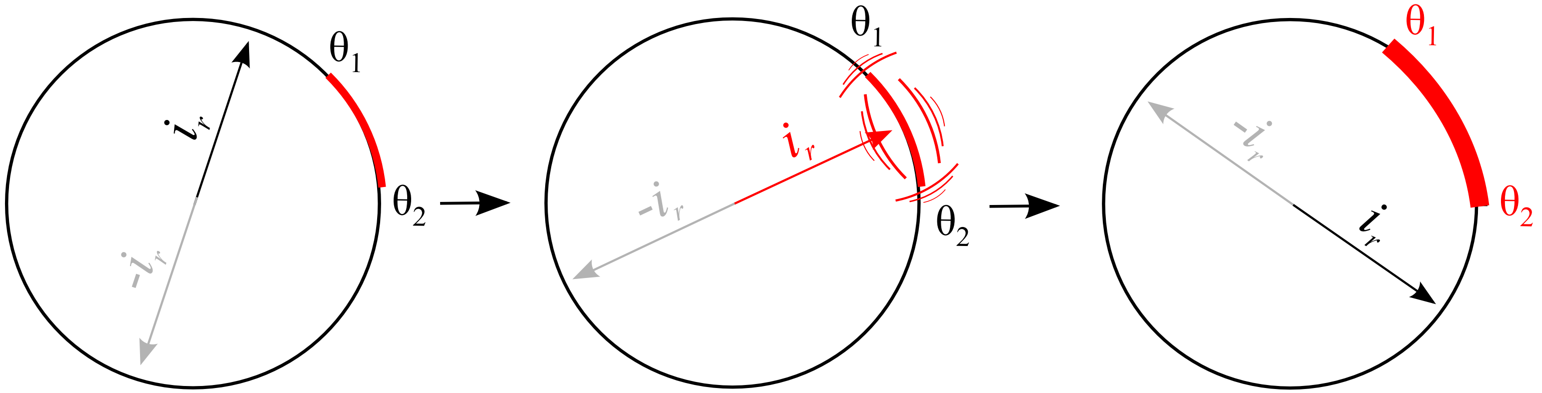

Transient leakage inductance

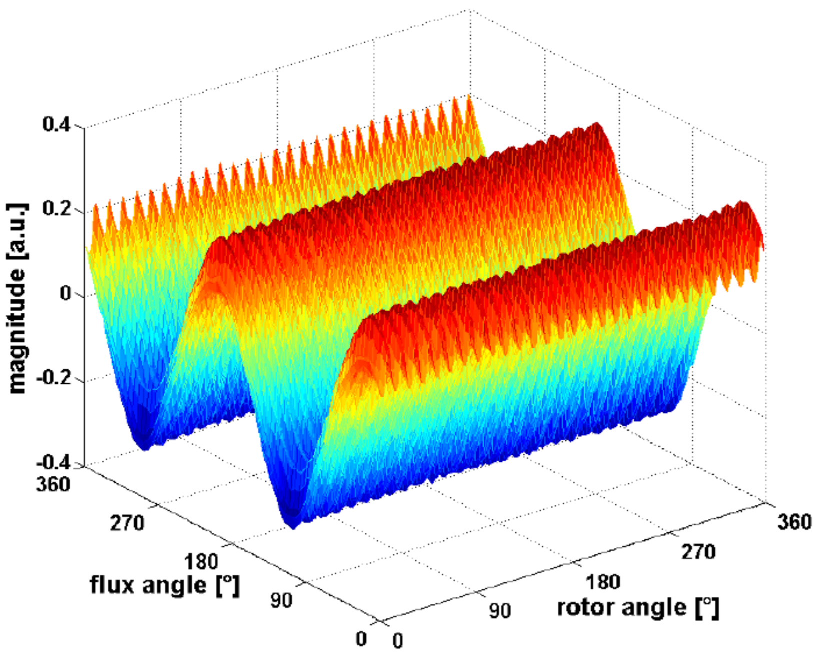

Healthy conditions

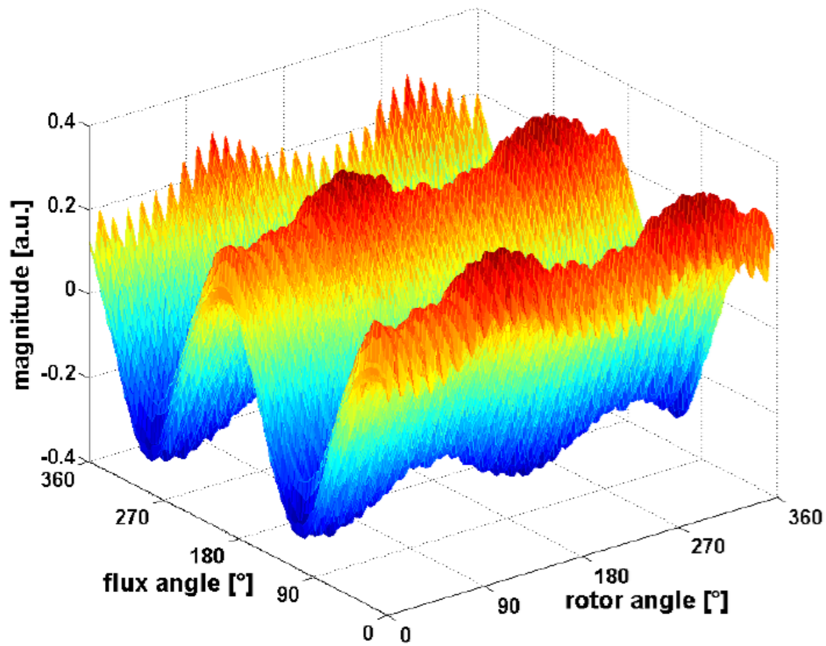

Damaged rotor bar

G. Stojčić et. al., "Separating Inherent Asymmetries from High Sensitivity Rotor Bar Fault Indicator", SDEMPED 2011

Upravljanje otporno na kvarove generatora

Fault-tolerant control

	Rotor cage defect:	Stator insulation fault:
Cause:	Cyclic thermal stress, bar-end-ring connection	Moisture, vibrations, thermal stress, PWM supply
Intervention:	Reduction of current flow through damaged cage part	Reduction of current flow through damaged insulation part
Methodology:	Torque modulation with frequency $2\omega_{sl}$	Stator flux modulation with frequency $2\omega_e$

Fault-tolerant control

	Rotor cage defect:	Stator insulation fault:
Cause:	Cyclic thermal stress, bar-end-ring connection	Moisture, vibrations, thermal stress, PWM supply
Intervention:	Reduction of current flow through damaged cage part	Reduction of current flow through damaged insulation part
Methodology:	Torque modulation with frequency $2\omega_{sl}$	Stator flux modulation with frequency $2\omega_e$

Fast loop: Modulation of torque/stator flux

Slow loop: Optimal power production

Cage defect fault-tolerant control

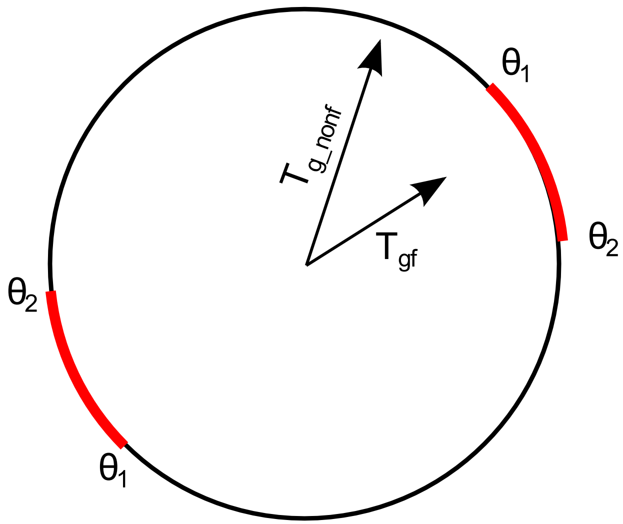

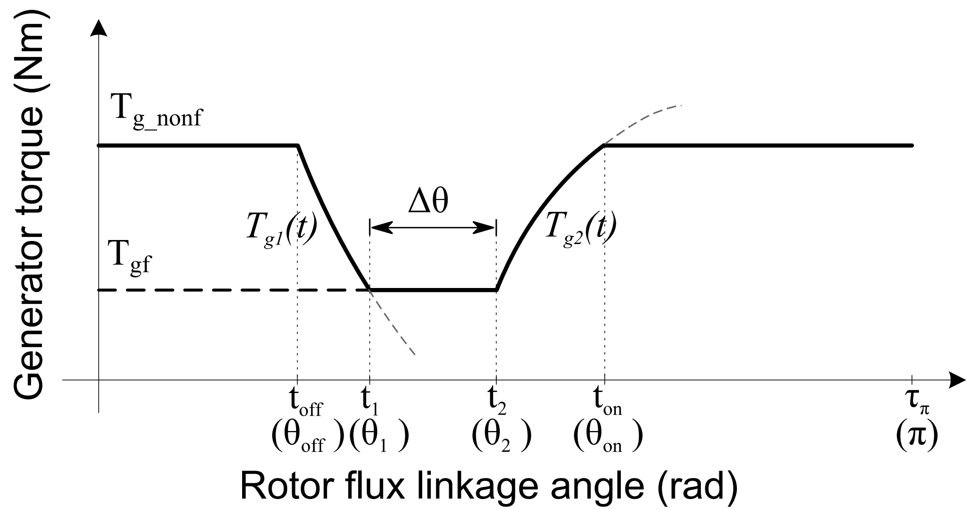

$$T_{g1}(t) = e^{-\frac{t}{\tau}}\left(T_{g\_nonf} - T_1\right) + T_1$$

$$T_{g2}(t) = T_2 - e^{-\frac{t}{\tau}}\left(T_2 - T_{gf}\right)$$

Cage defect fault-tolerant control

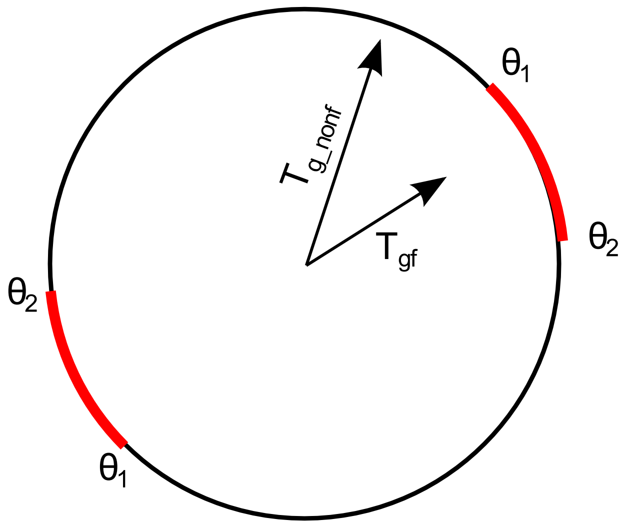

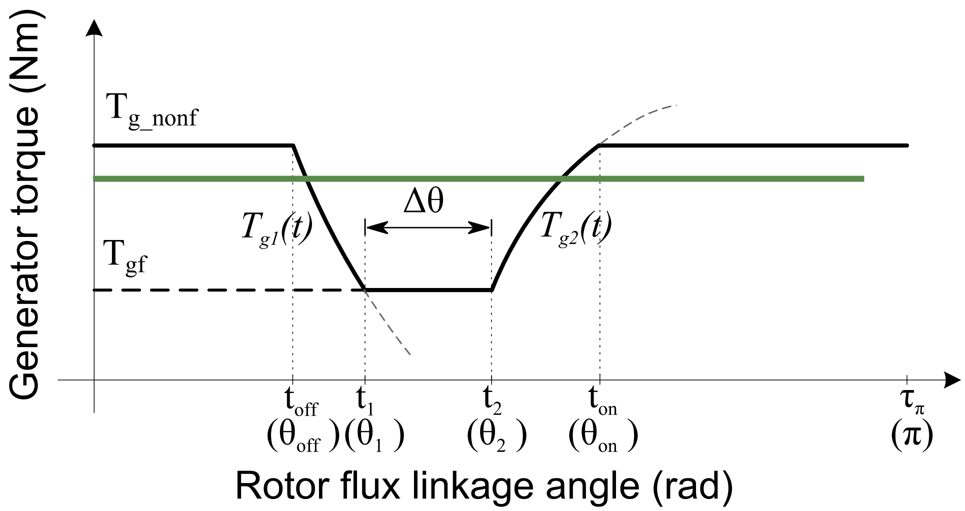

$$T_{g1}(t) = e^{-\frac{t}{\tau}}\left(T_{g\_nonf} - T_1\right) + T_1$$

$$T_{g2}(t) = T_2 - e^{-\frac{t}{\tau}}\left(T_2 - T_{gf}\right)$$

Mean torque = optimum torque

Operating area under fault

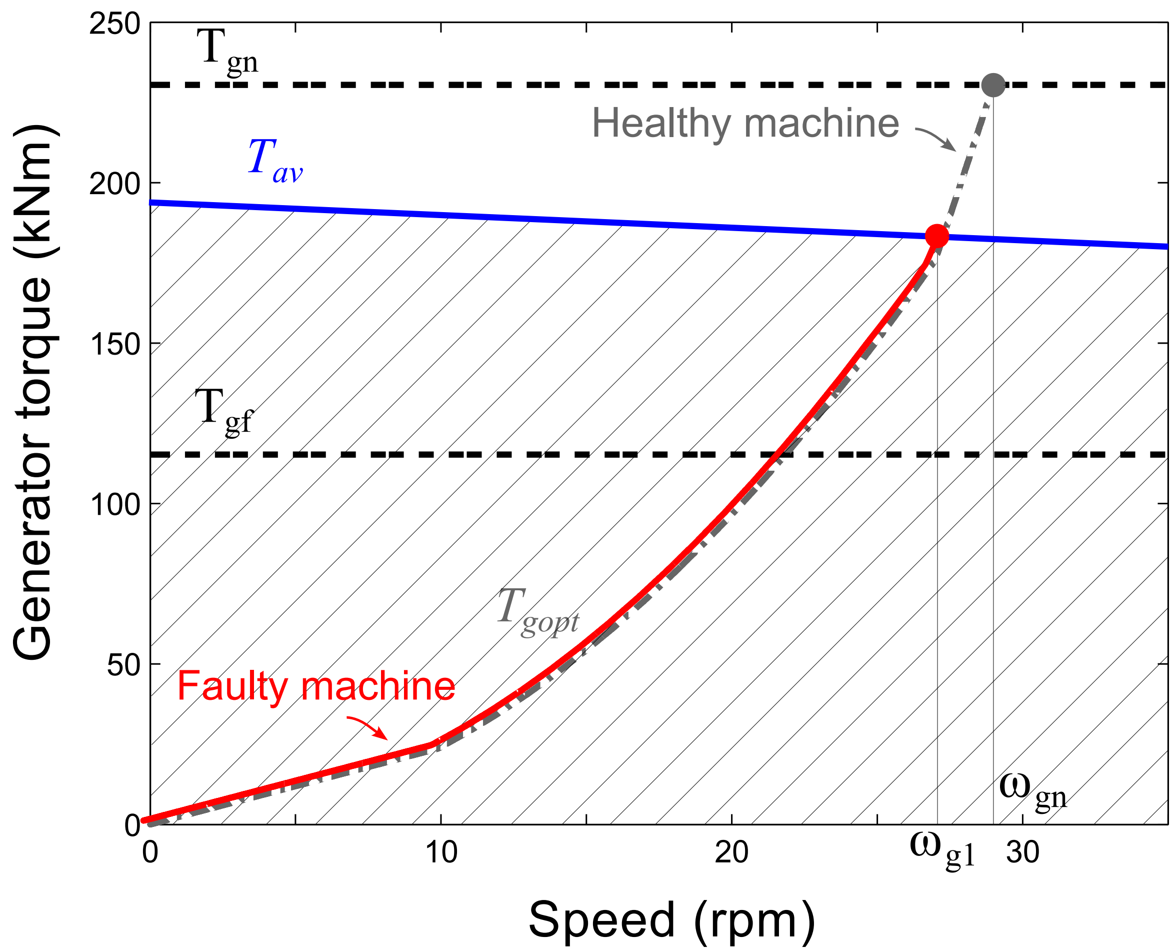

WT 700 kW

Extension of WT control

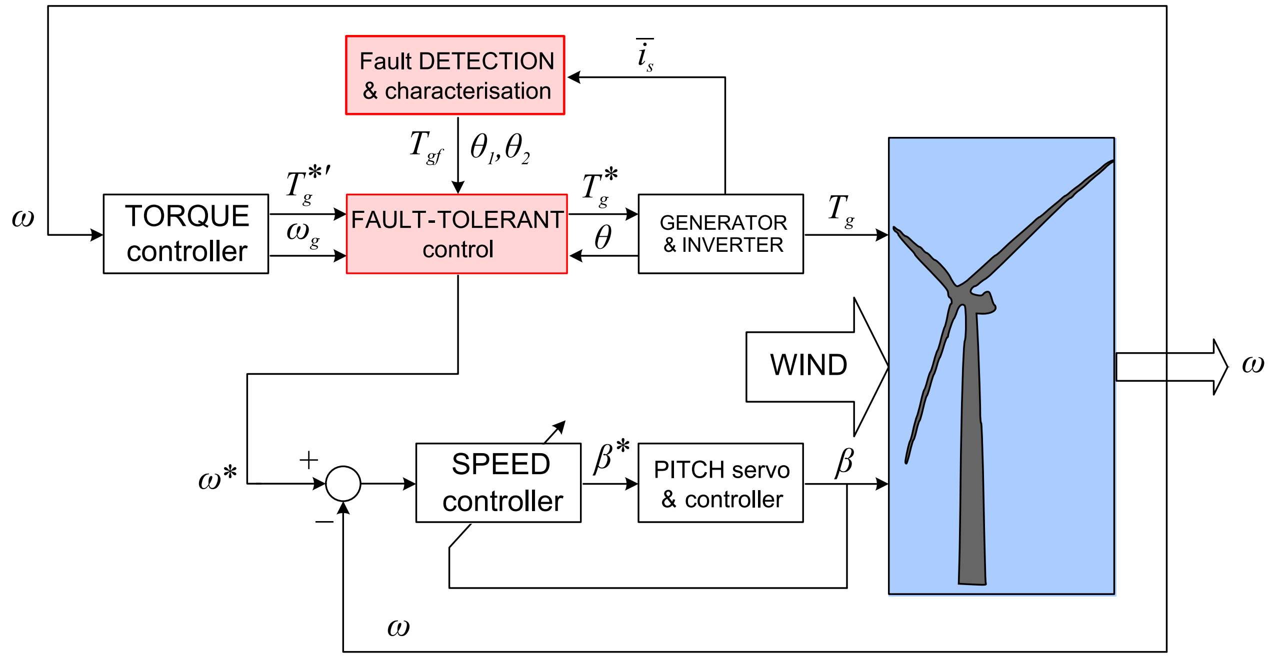

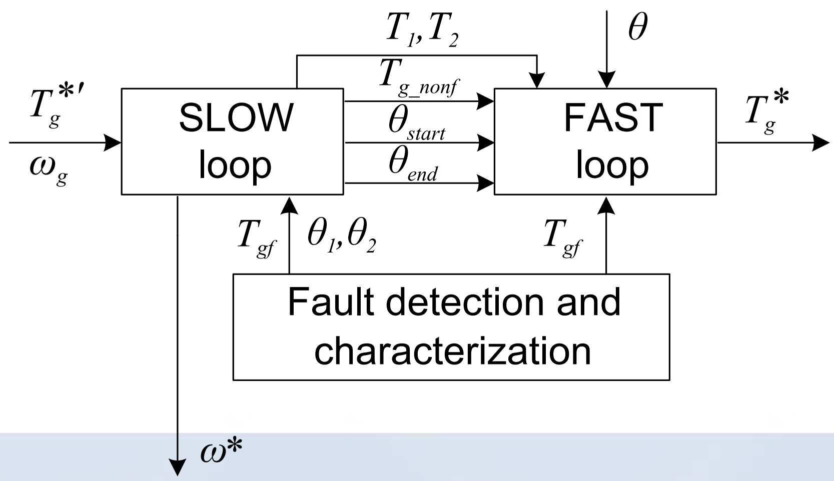

Simulation results

Cage defect simulated at t=50 s

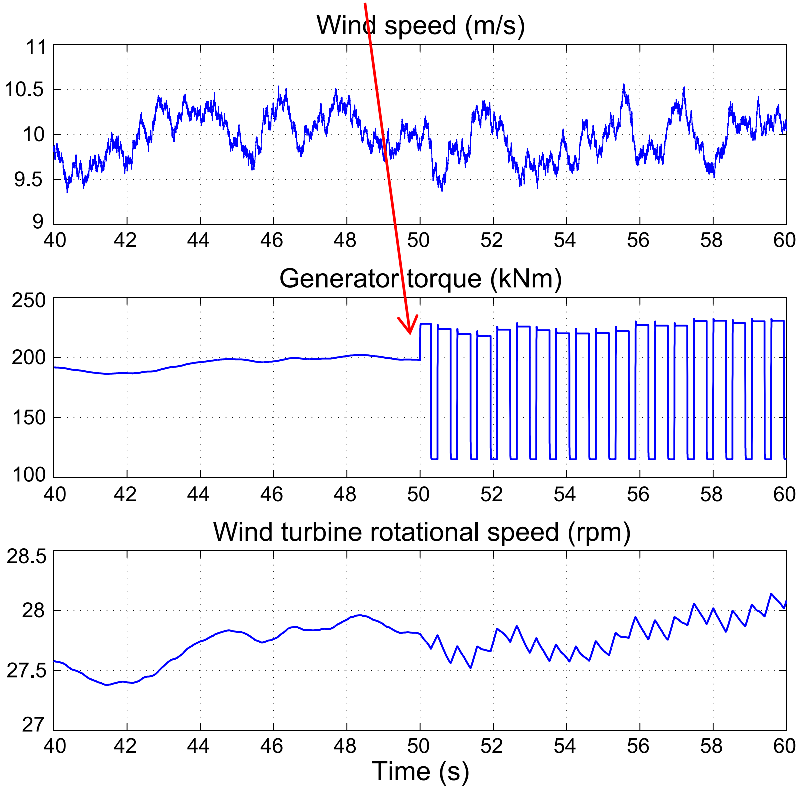

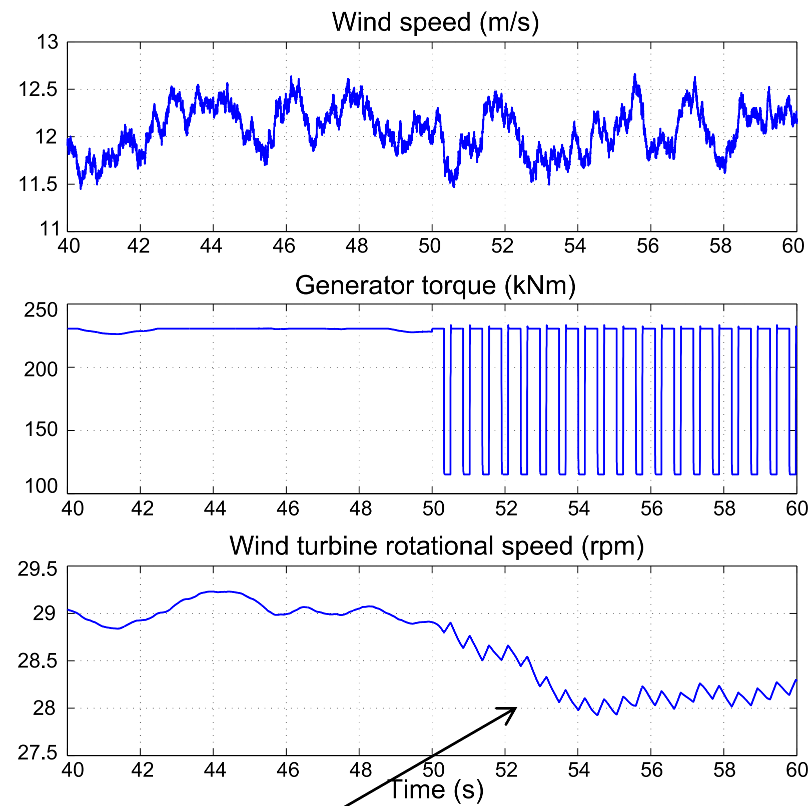

Lowered rated speed

Experimental setup

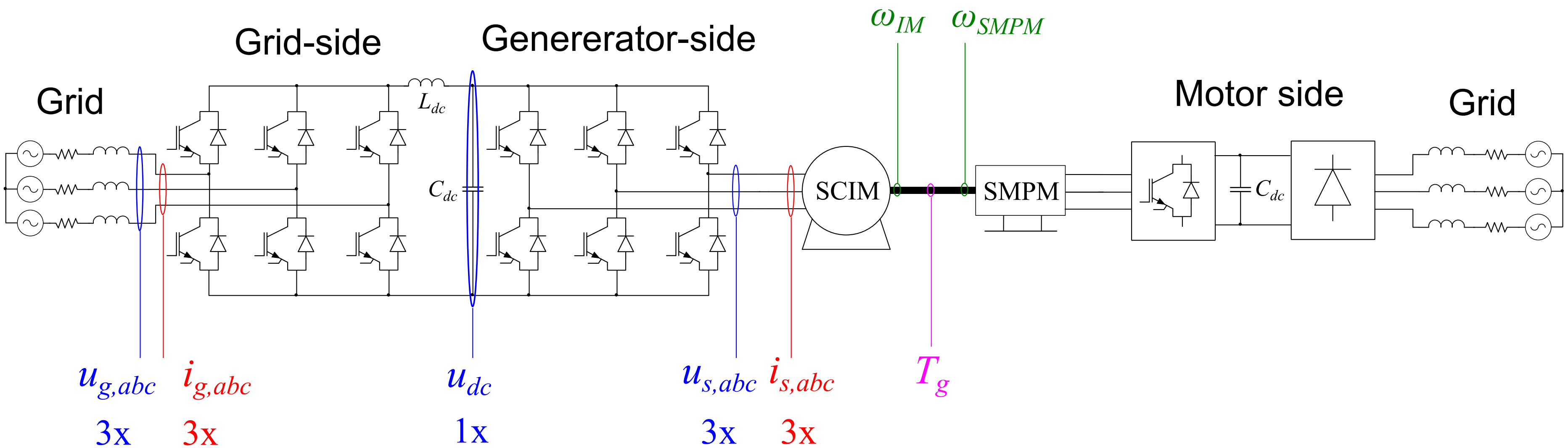

Experimental setup

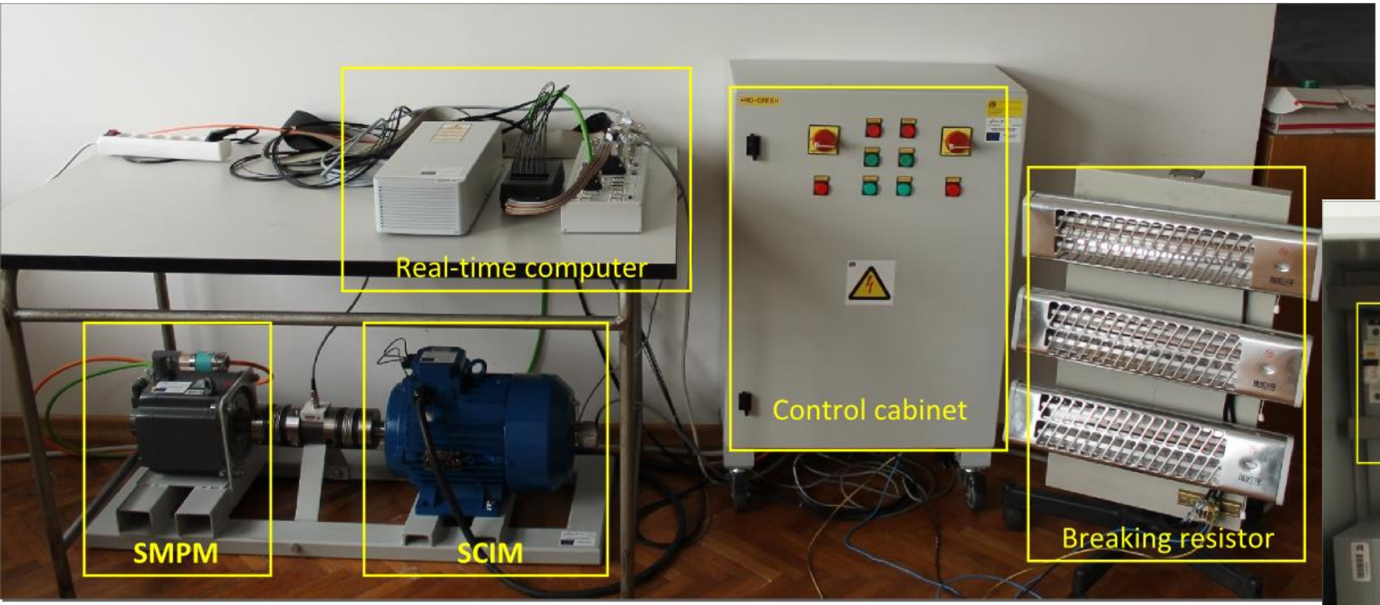

Control cabinet

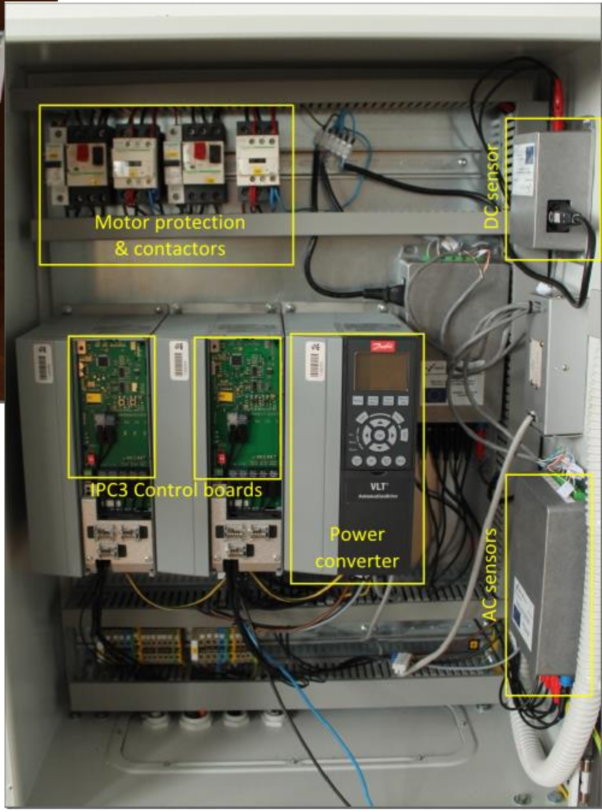

dSPACE 1103

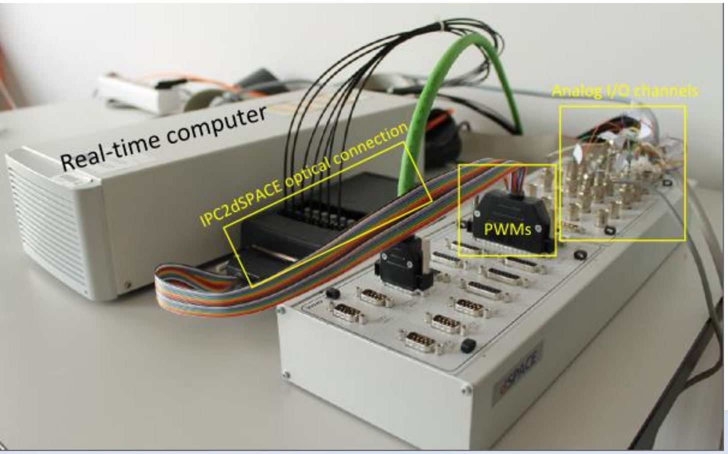

ControlDesk software

Experimental setup

Description	Parameter	Value
Rated power	P_{gn}	5.5 kW
Rated voltage	U_n	400 V
Rated current	I_n	11 A
Rated frequency	f_n	50 Hz
Number of pole pairs	p	2
Rated speed (generator)	ω_{gn}	1435 rpm
Rated torque	T_{gn}	36.6 Nm
Stator resistance	R_s	0.6193 Ω
Rotor resistance	R_r	0.5093 Ω
Stator inductance	L_s	0.1804 H
Rotor inductance	L_r	0.1807 H
Mutual inductance	L_m	0.1738 H
Rated rotor flux magnitude	ψ_{rdn}	0.8444 Wb
Rated stator flux magnitude	ψ_{sn}	0.8989 Wb
Total moment of inertia (datasheets)	J_g	0.0383 kgm^2
Delta connected	Δ	

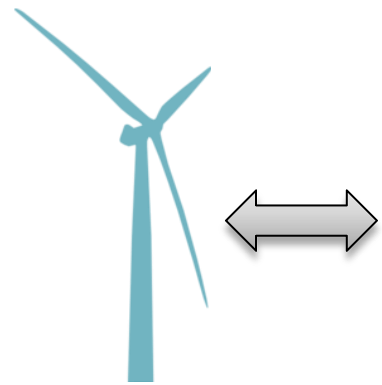

Parameter	Value	
P_n	Rated power	700 kW
T_{tn}	Rated turbine torque	230.5 kNm
ω_n	Rated rotor speed	3.0369 rad/s (29 rpm)
C_{Pmax}	Rated turbine torque	0.4745
λ_{opt}	Optimal tip-speed-ratio	7.4
K_λ	Torque loop constant	$2.2 \cdot 10^4$ kgm^2
β_0	Minimum pitch angle	$-1°$
J_t	WT moment of inertia	776215 kgm^2
ρ_{air}	Air density	1.225 kg/m^3
R	Radius of WT rotor	25 m
h_{tower}	Tower height	50 m
M	Tower modal mass	51020 kg
D	Tower damping coefficient	2215.7
C	Tower stiffness coefficient	9622.3

Experimental results

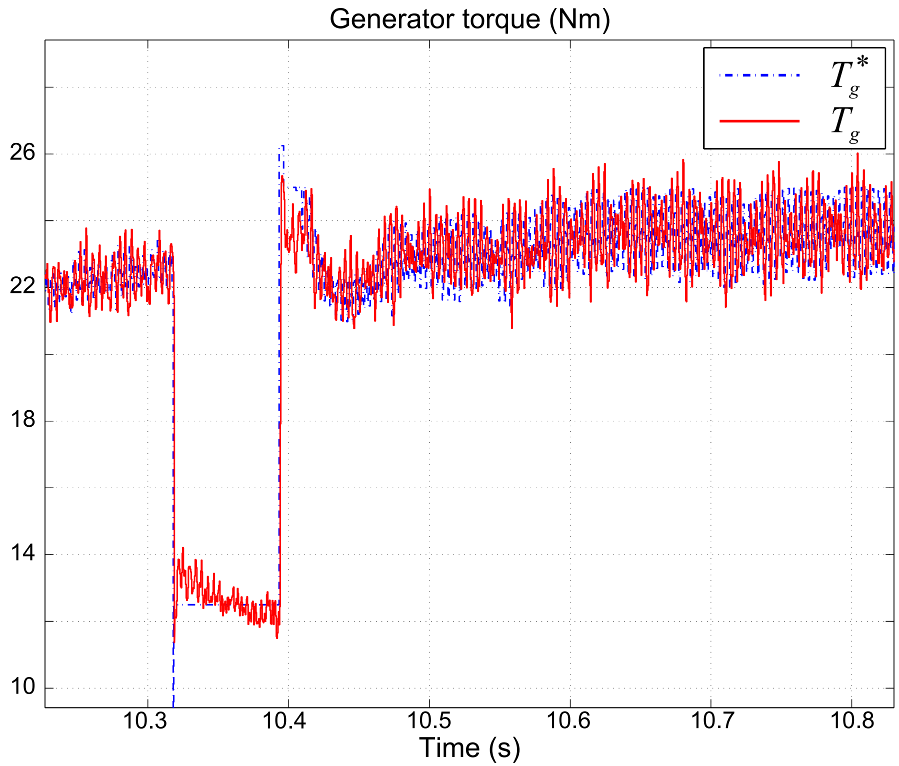

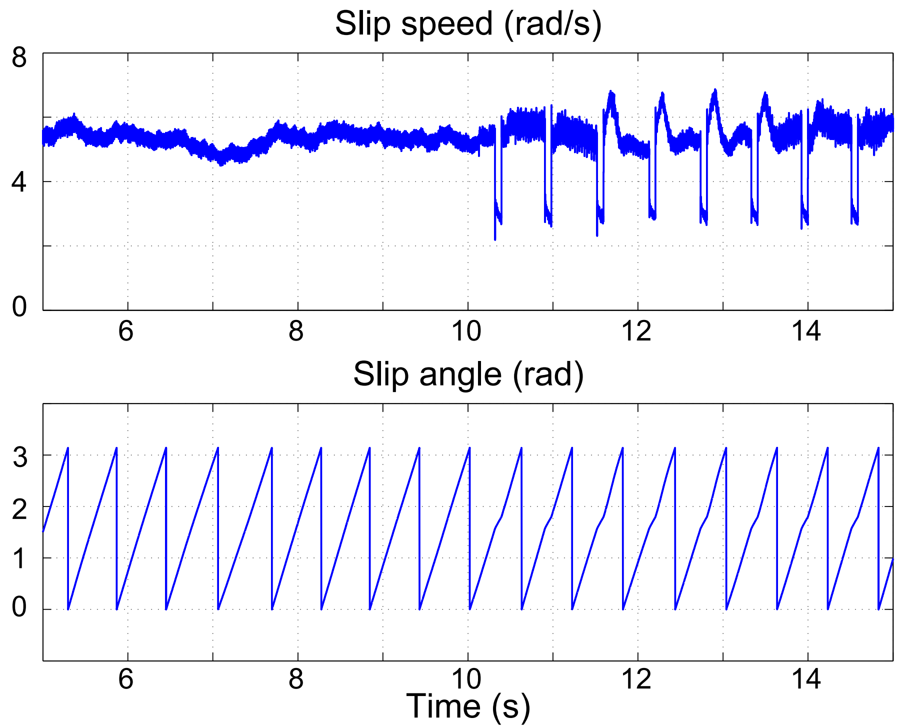

Stator insulation FTC

Inter-turn short circuit

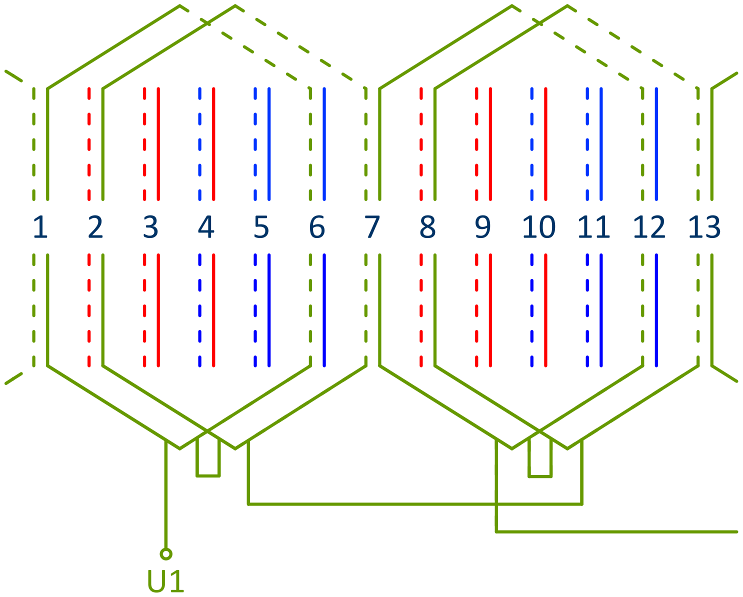

Stator insulation FTC

Inter-turn short circuit

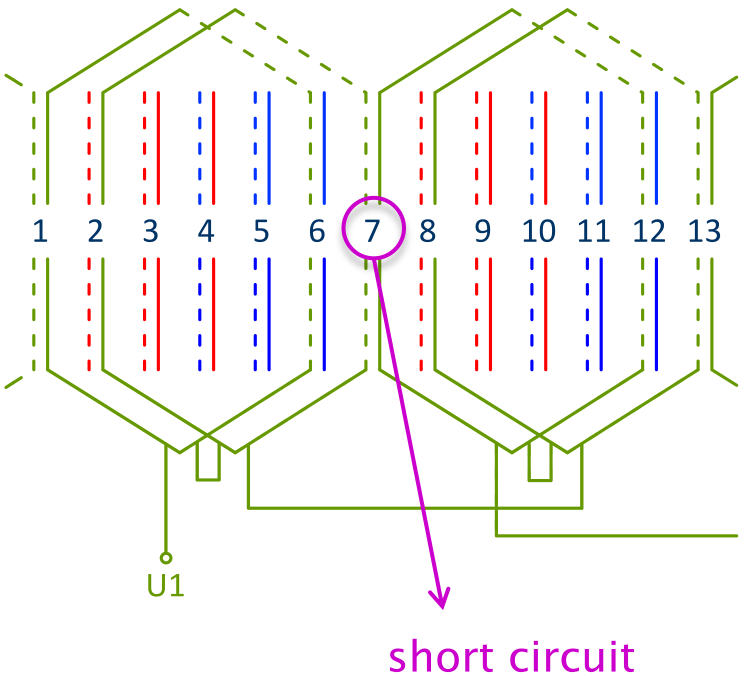

Stator insulation FTC

Inter-turn short circuit

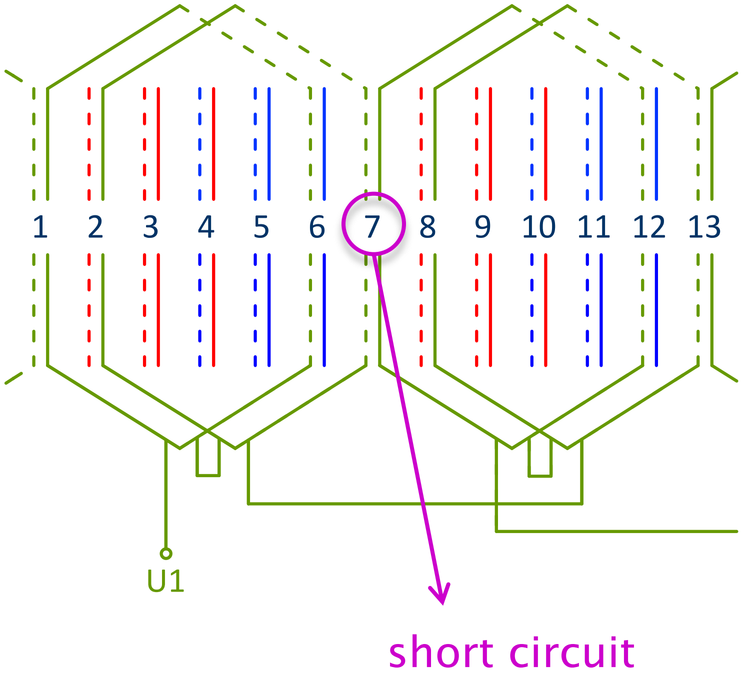

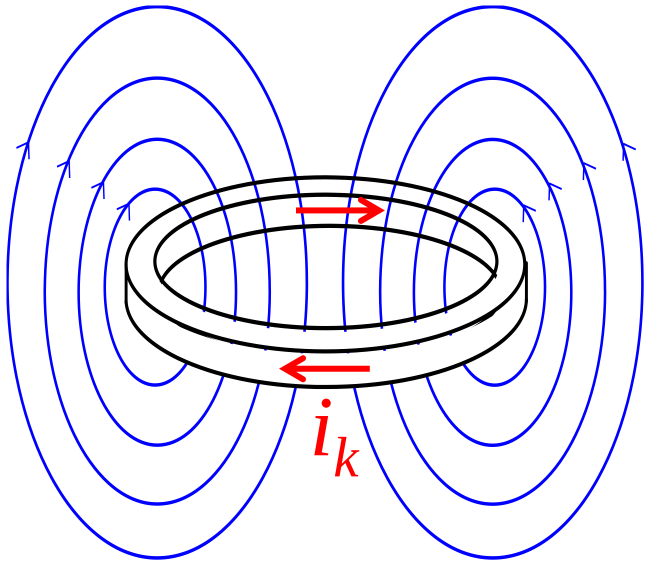

Stator insulation FTC

Inter-turn short circuit

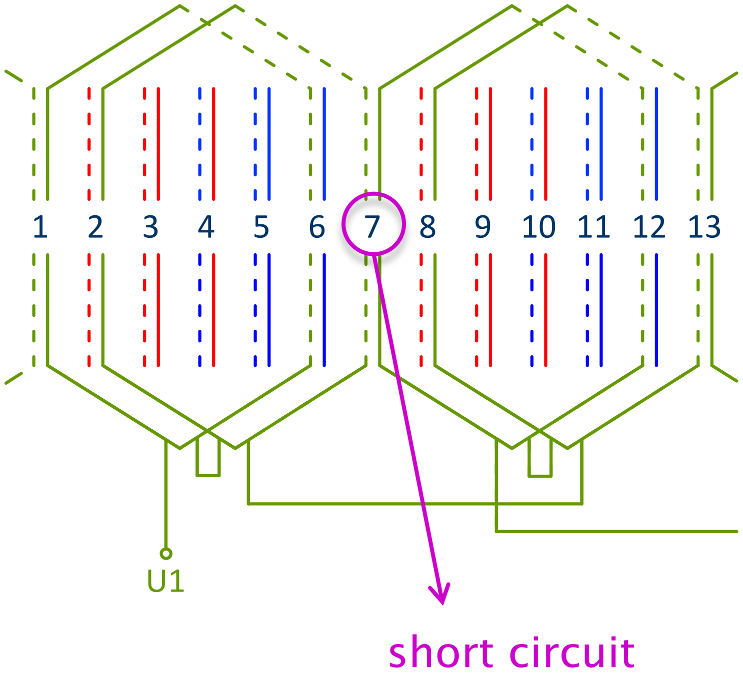

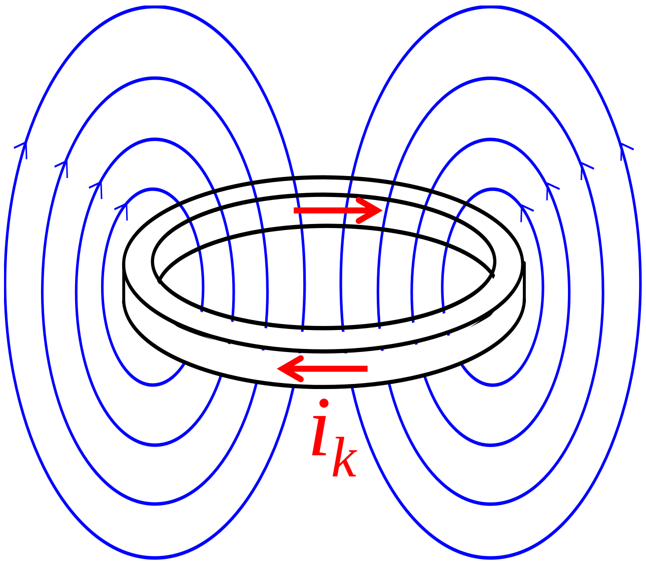

$$i_k(t) = \frac{1}{Z_k} \frac{d\psi_{sx}(t)}{dt}$$

Stator insulation FTC

Inter-turn short circuit

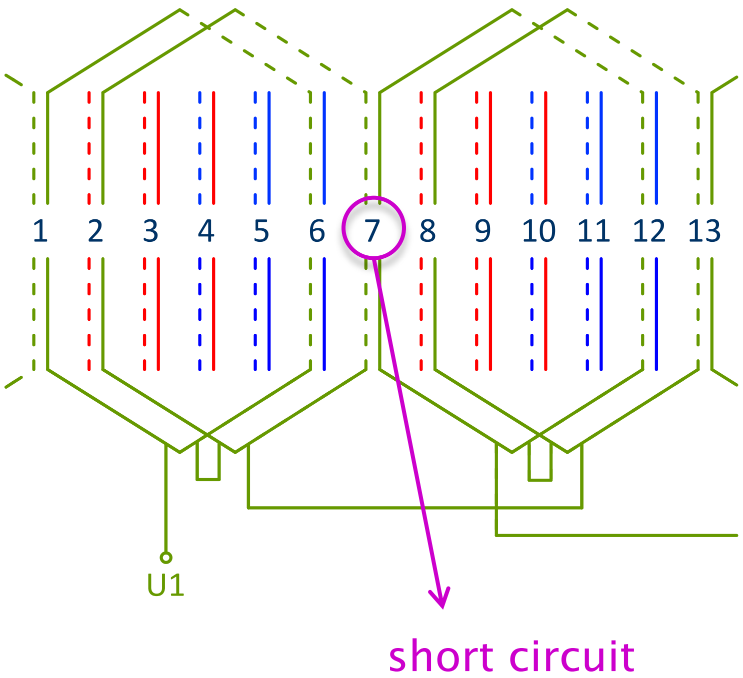

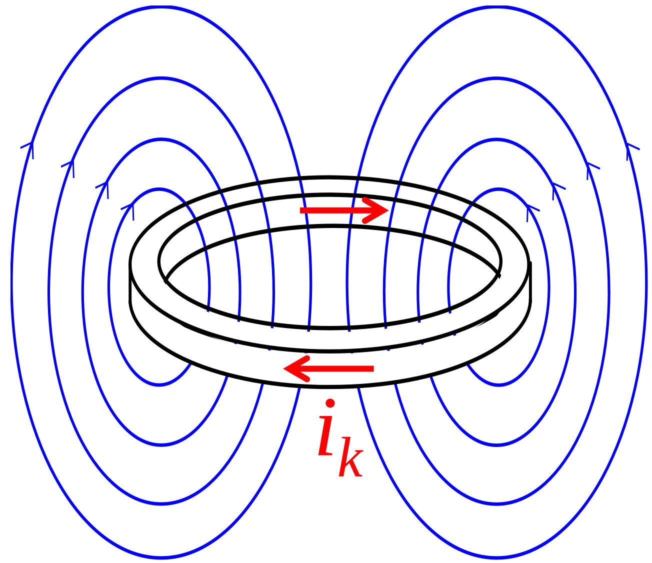

$$i_k(t) = \frac{1}{Z_k} \frac{d\psi_{sx}(t)}{dt}$$

$$\Rightarrow \left| \frac{d\psi_{sx}(t)}{dt} \right| \leq K_{FTC}$$

Stator insulation FTC

Degraded insulation

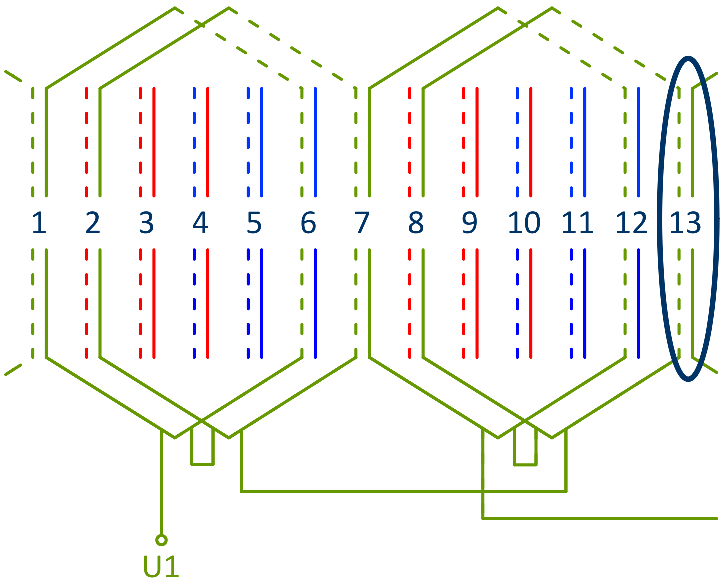

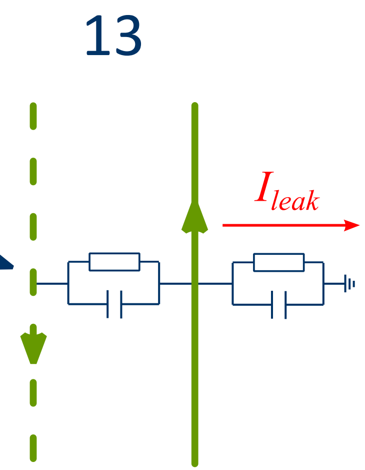

Stator insulation FTC

Degraded insulation

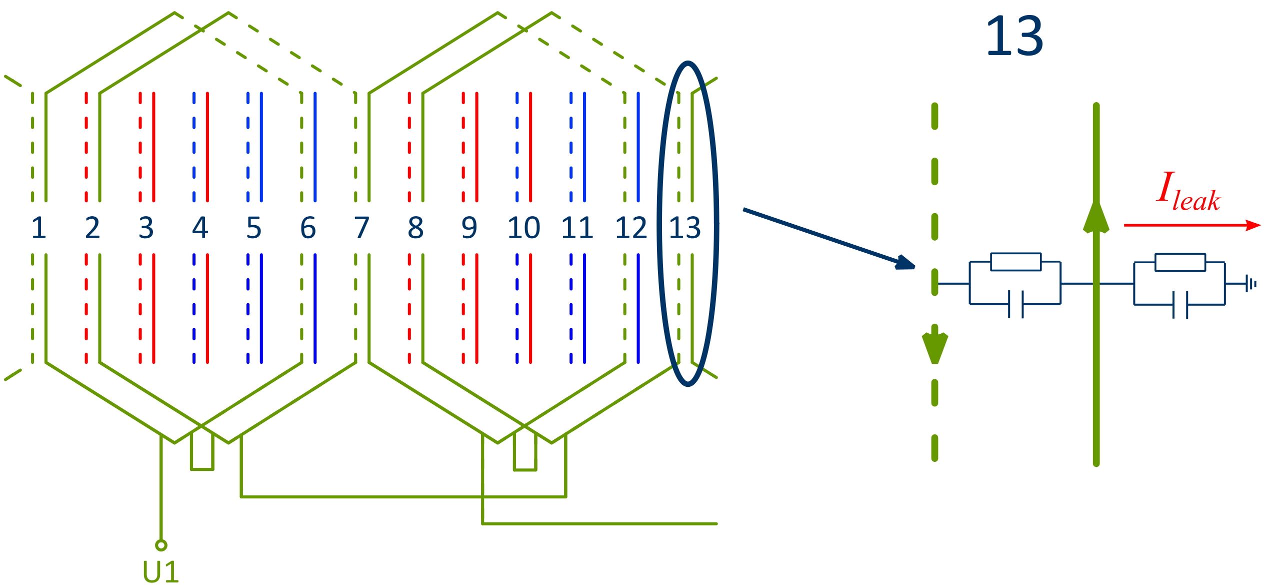

J. Yang et. al., “An advanced stator winding insulation quality assessment technique for inverter-fed machines”, TIA 2008.

Healthy insulation

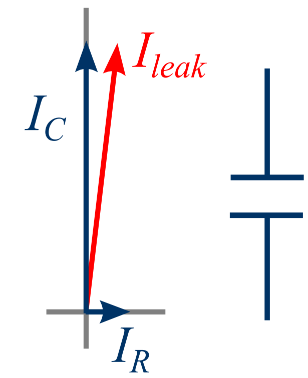

$$i_{leak}(t) = C\frac{du_{sx}(t)}{dt}$$

Stator insulation FTC

Degraded insulation

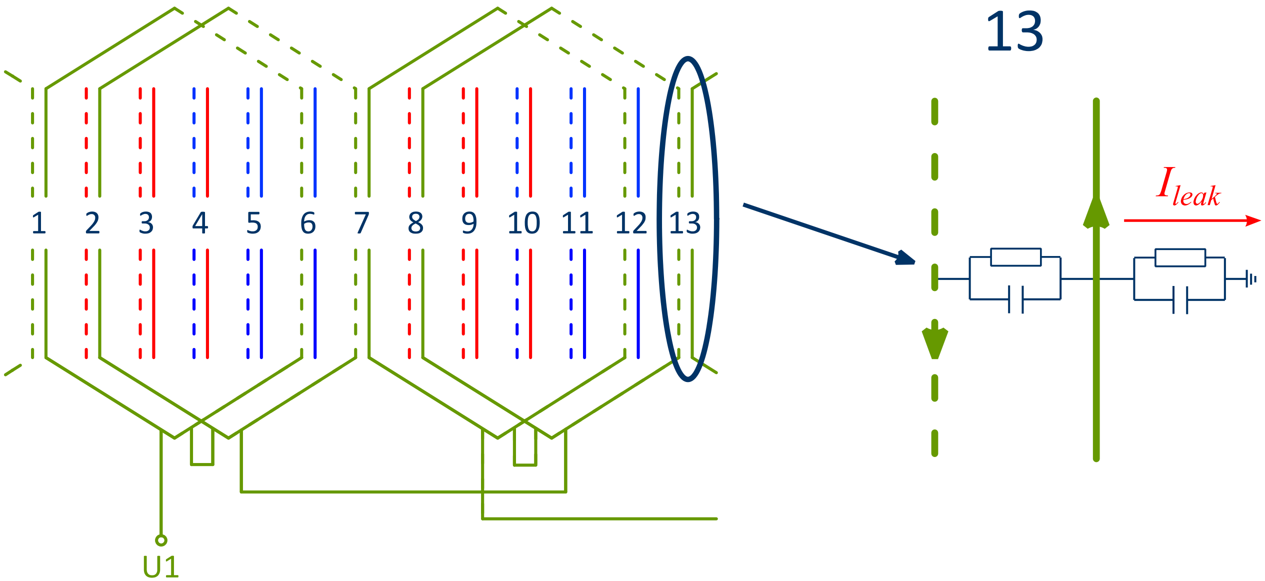

J. Yang et. al., “An advanced stator winding insulation quality assessment technique for inverter-fed machines”, TIA 2008.

Healthy insulation

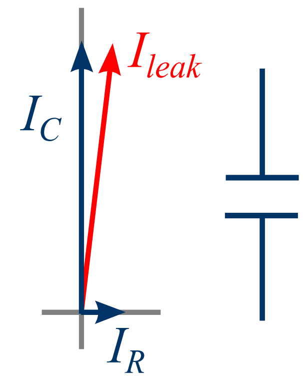

$$i_{leak}(t) = C\frac{du_{sx}(t)}{dt}$$

Degraded insulation

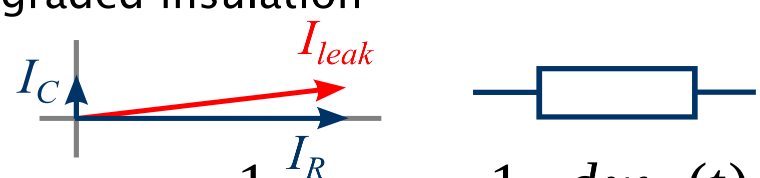

$$i_{leak}(t) = \frac{1}{R}u_{sx}(t) \approx \frac{1}{R}\cdot\frac{d\psi_{sx}(t)}{dt}$$

Stator insulation FTC

Degraded insulation

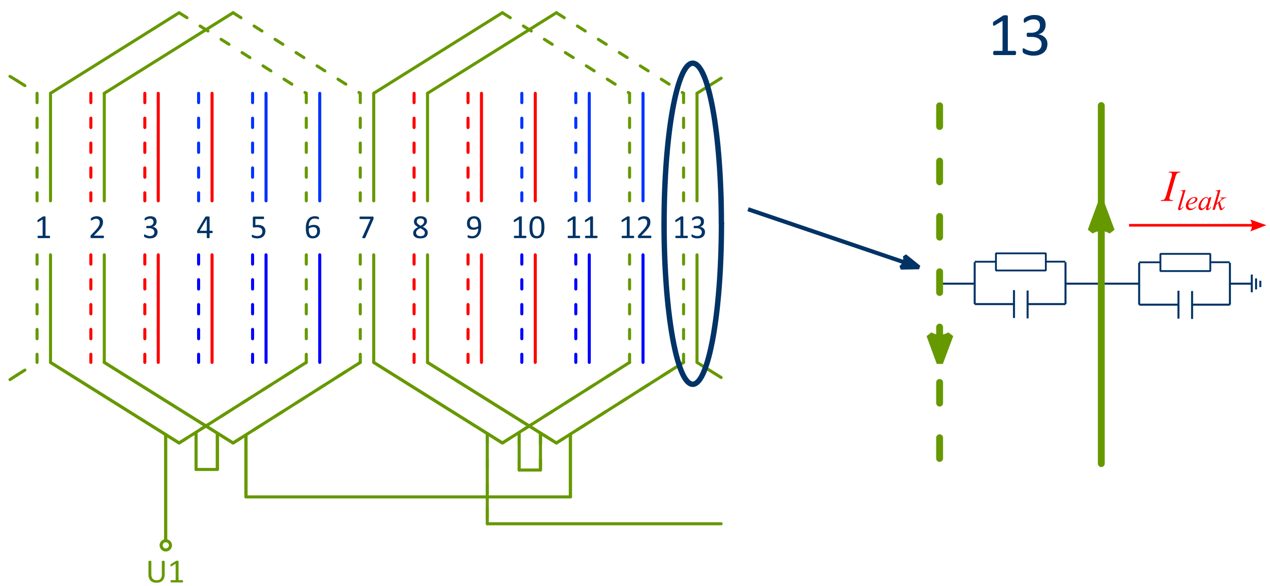

J. Yang et. al., “An advanced stator winding insulation quality assessment technique for inverter-fed machines”, TIA 2008.

Healthy insulation

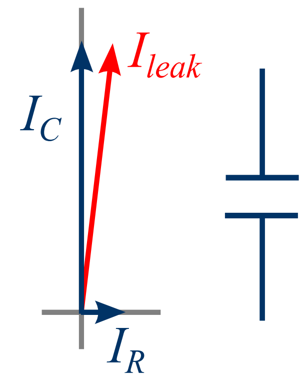

$$i_{leak}(t) = C\frac{du_{sx}(t)}{dt}$$

Degraded insulation

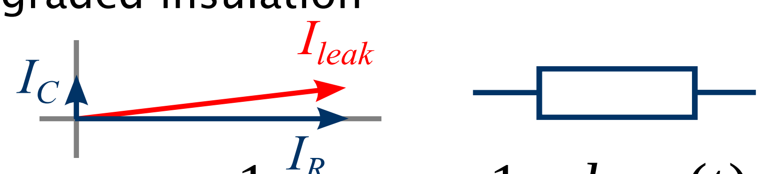

$$i_{leak}(t) = \frac{1}{R}u_{sx}(t) \approx \frac{1}{R}\cdot\frac{d\psi_{sx}(t)}{dt}$$

$$\left|\frac{d\psi_{sx}(t)}{dt}\right| \le K_{FTC}$$

Stator insulation FTC

- Generally:

$$\psi_{sx}(t) = |\psi_s| \sin(\omega_e t + \varphi_x)$$

$$\frac{d\psi_{sx}(t)}{dt} = |\psi_s| \omega_e \cos(\omega_e t + \varphi_x)$$

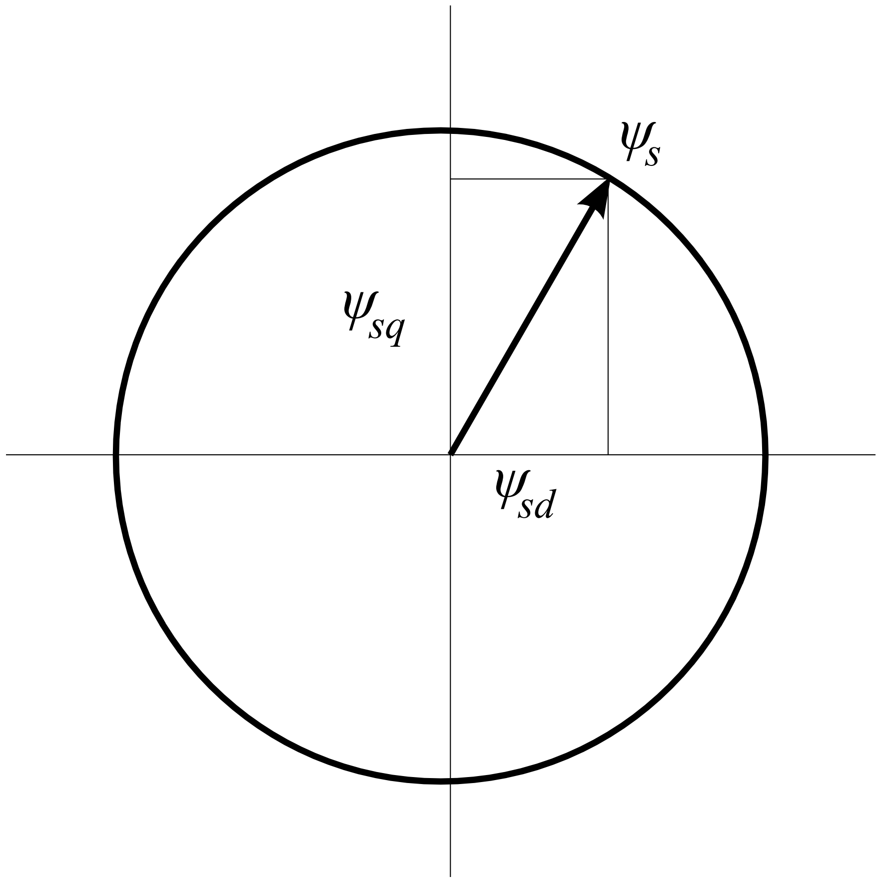

Stator insulation FTC

- Option A – reduction of ψ_s such that $|\psi_s|\omega_e$ is kept below the imposed limit

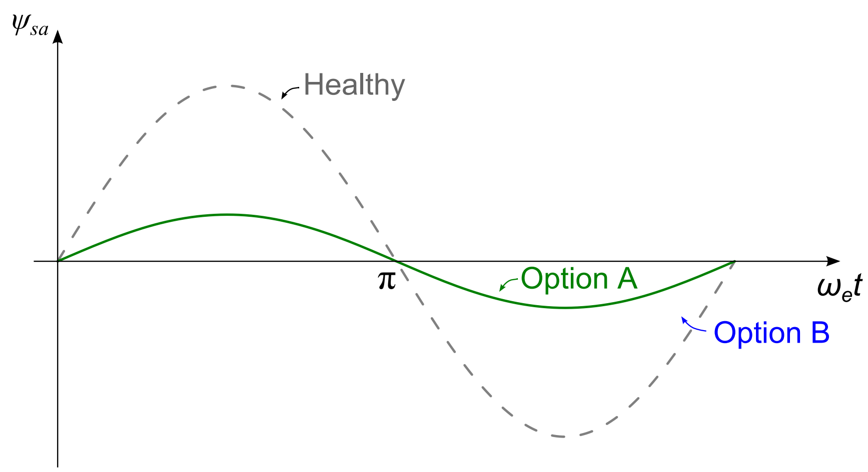

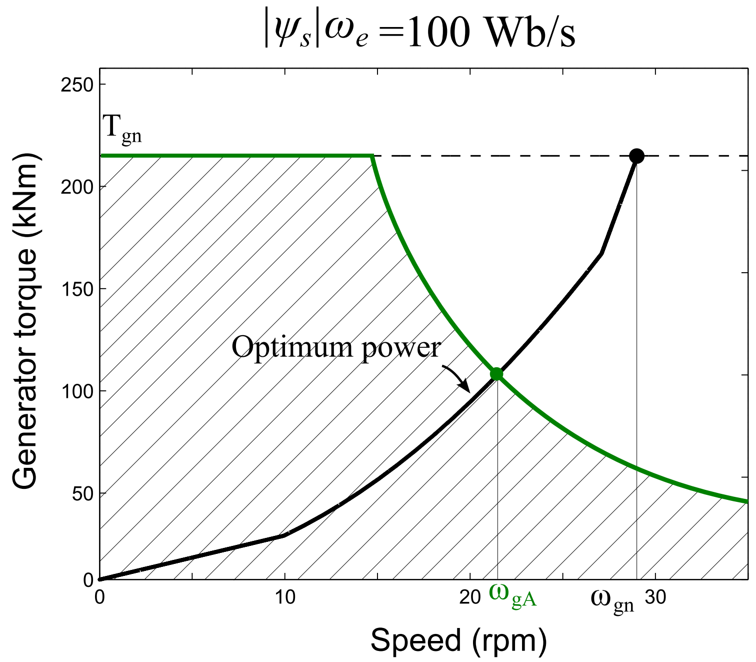

Stator insulation FTC

- Option B – modulation of stator flux magnitude $|\psi_s|(t)$ such that the imposed restriction is matched

$$\left|\frac{d\psi_{sx}(t)}{dt}\right| = K_{FTC}$$

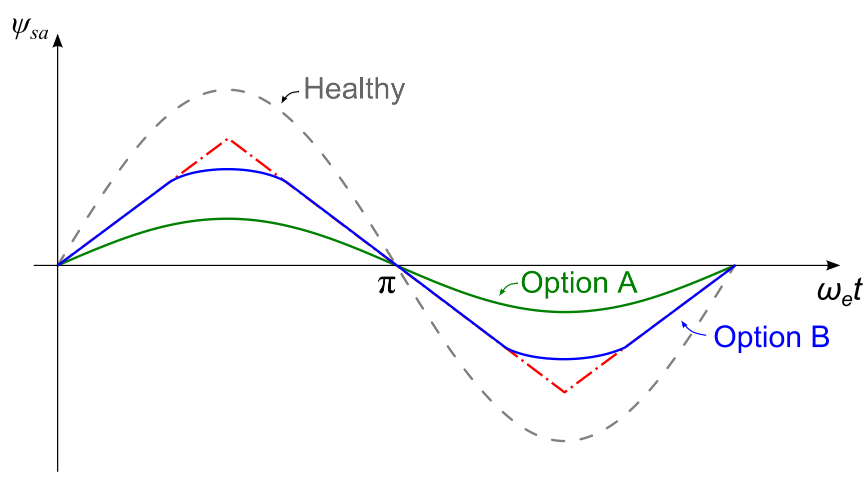

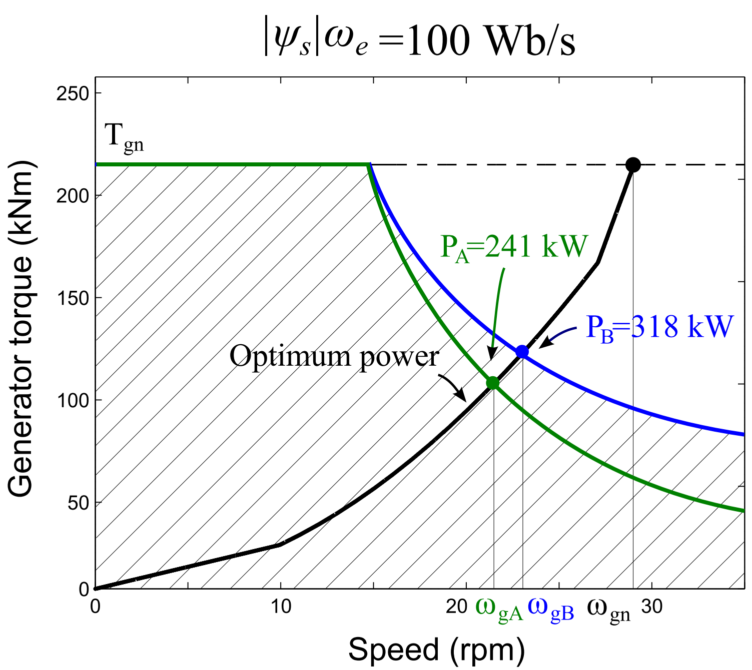

Stator insulation FTC

- Triangular waveform of stator flux is achieved with FOC and current control loops:

$$|\psi_{sx}|(t) = \frac{K_{FTC}}{\omega_e} \frac{\omega_e t + \varphi_x}{\sin(\omega_e t + \varphi_x)} \Rightarrow \psi_{sx}(t) = K_{FTC}\left(t + \frac{\varphi_x}{\omega_e}\right)$$

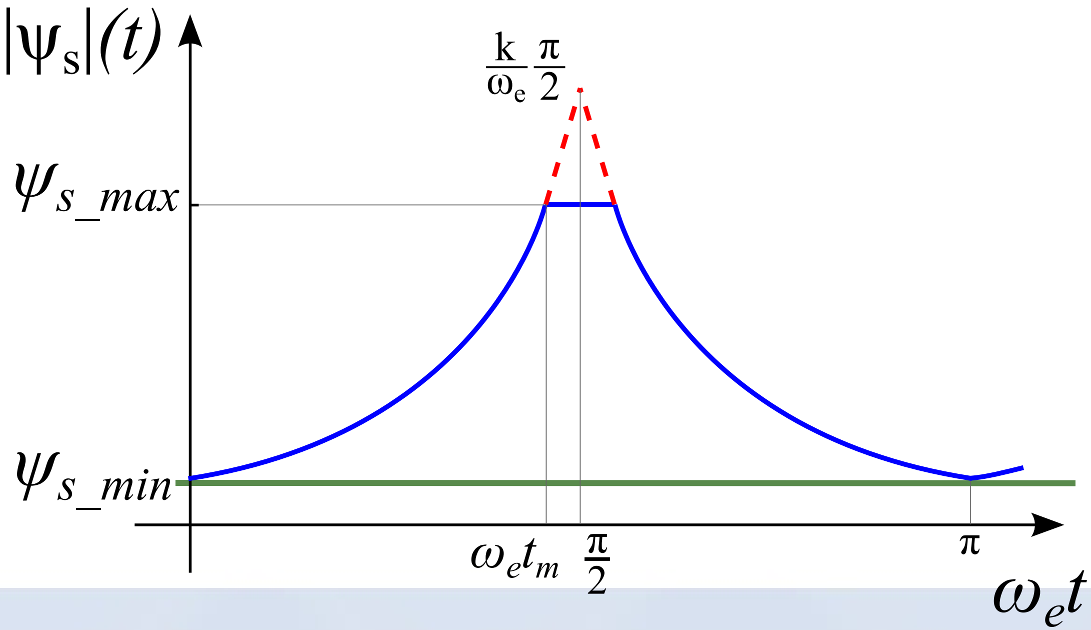

Stator insulation FTC

- Triangular waveform of stator flux is achieved with FOC and current control loops:

$$\left|\psi_{sx}\right|(t) = \frac{K_{FTC}}{\omega_e}\frac{\omega_e t + \varphi_x}{\sin(\omega_e t + \varphi_x)} \quad \Rightarrow \quad \psi_{sx}(t) = K_{FTC}\left(t + \frac{\varphi_x}{\omega_e}\right)$$

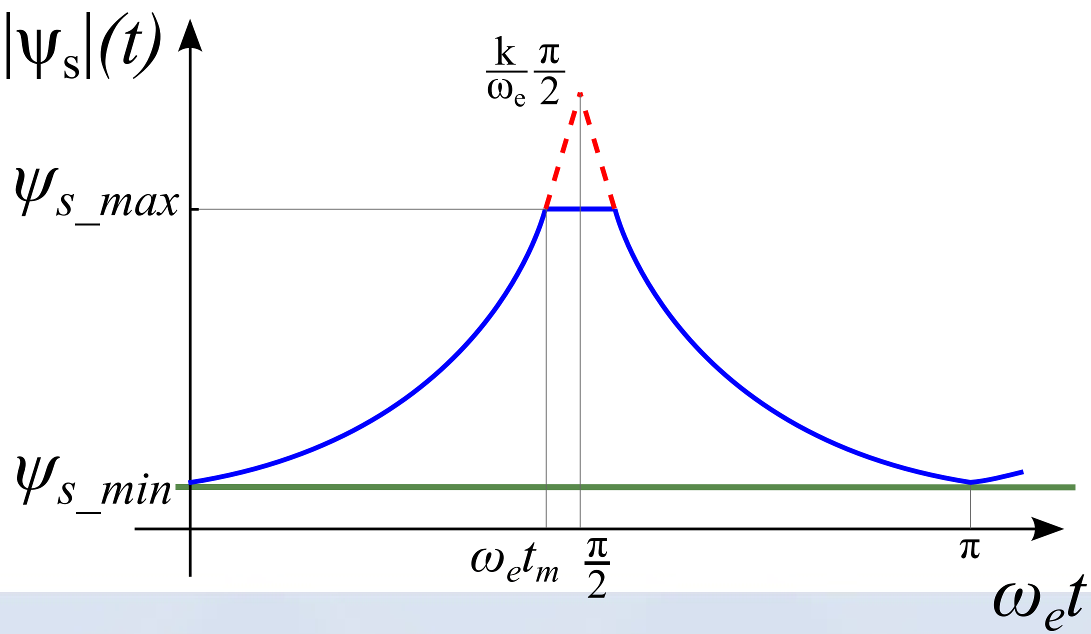

$$\psi_{sd} = L_l i_{sd} + \frac{L_m}{L_r}\psi_{rd}$$

$$\psi_{sq} = L_l i_{sq}$$

$$\psi_{rd} \approx konst.$$

$$\omega_{sl} = \omega_{sln}$$

Stator flux modulation

- Periodic strengthening and weakening of machine flux in the air gap

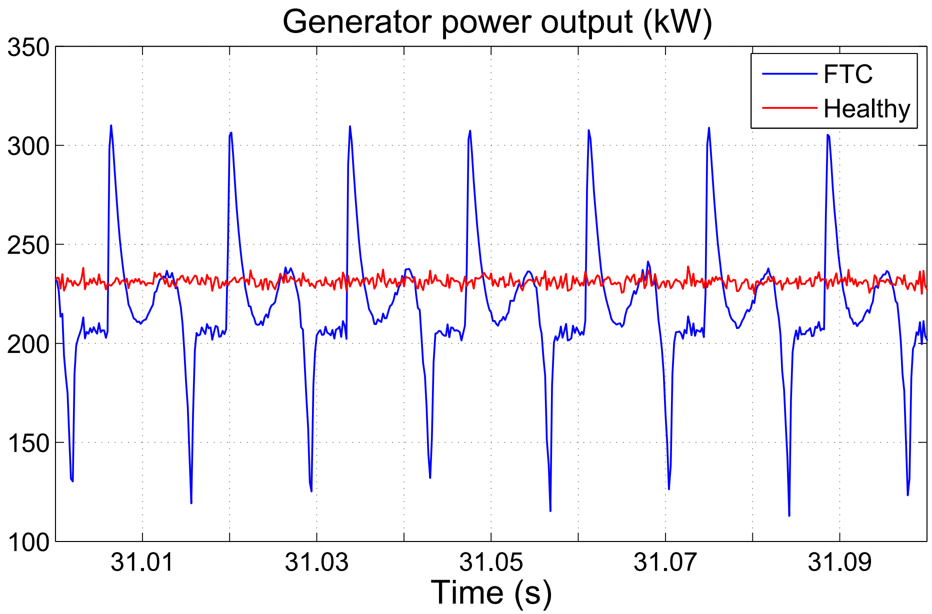

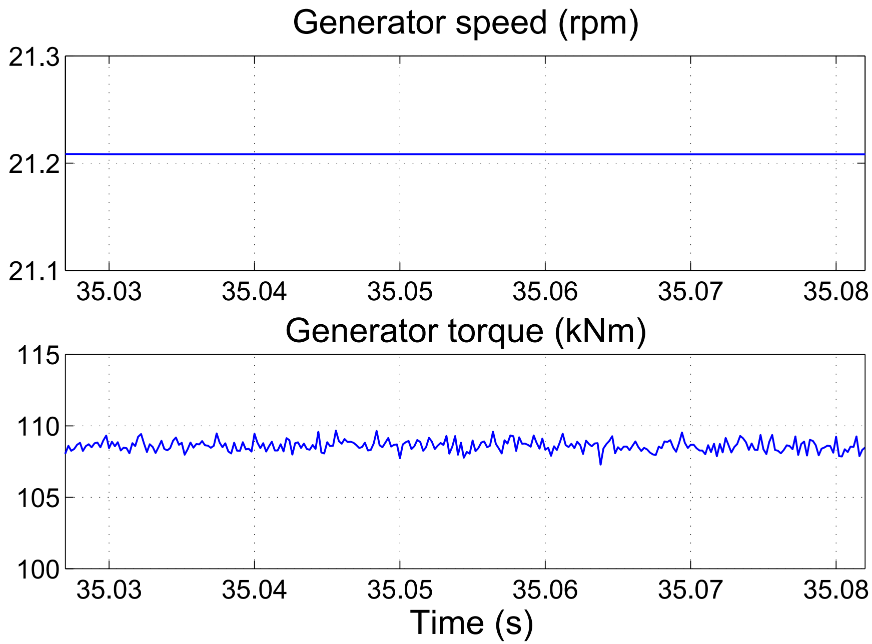

Extension of WT control

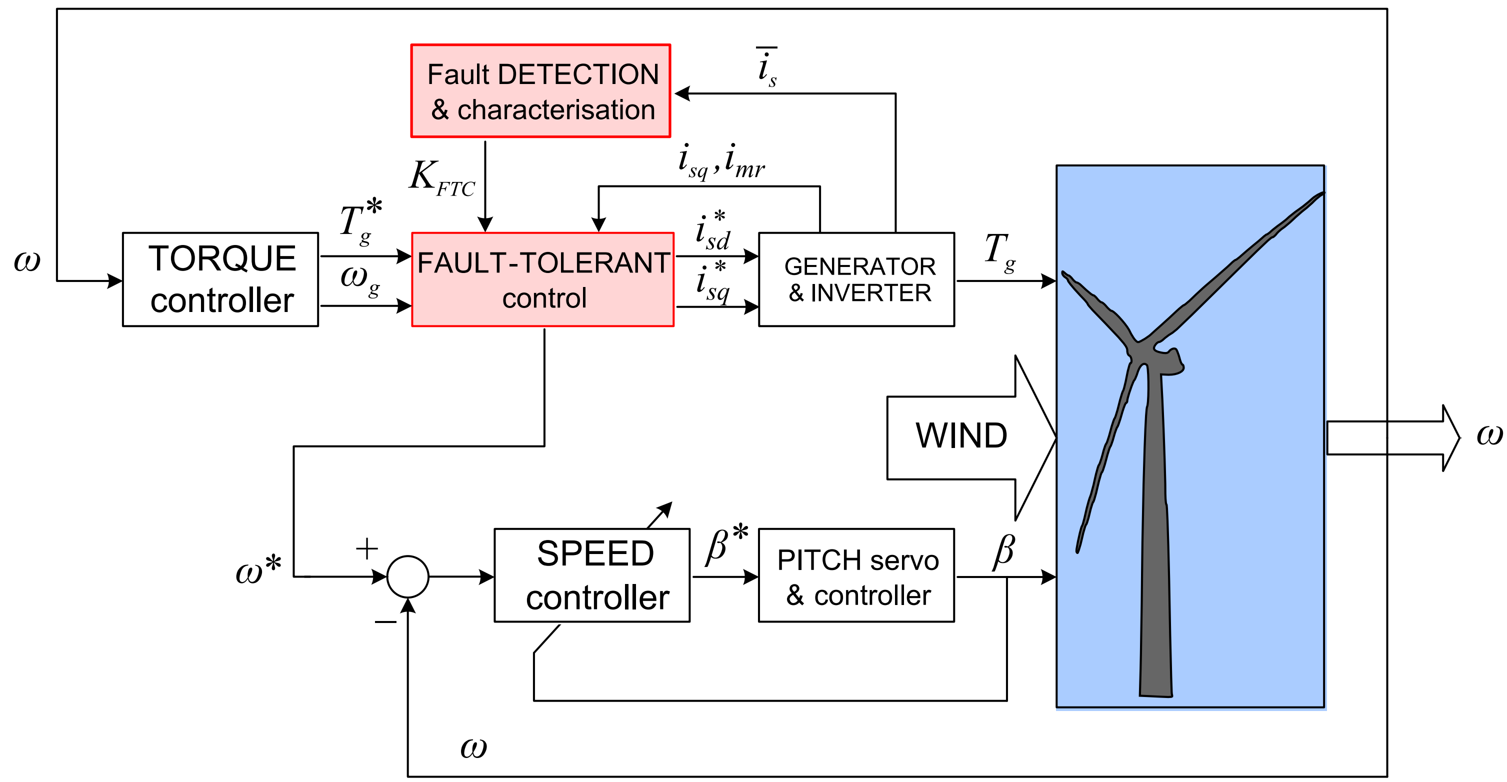

Simulation results

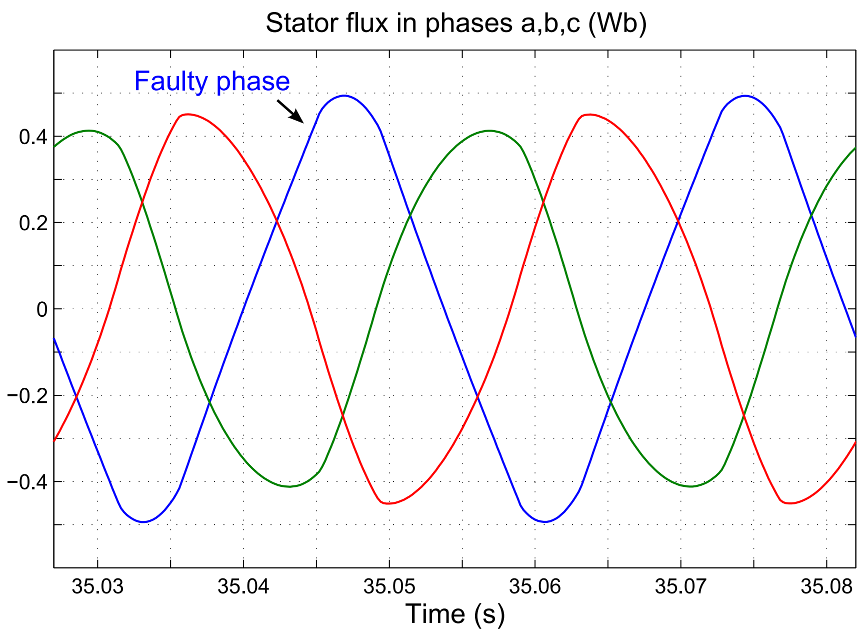

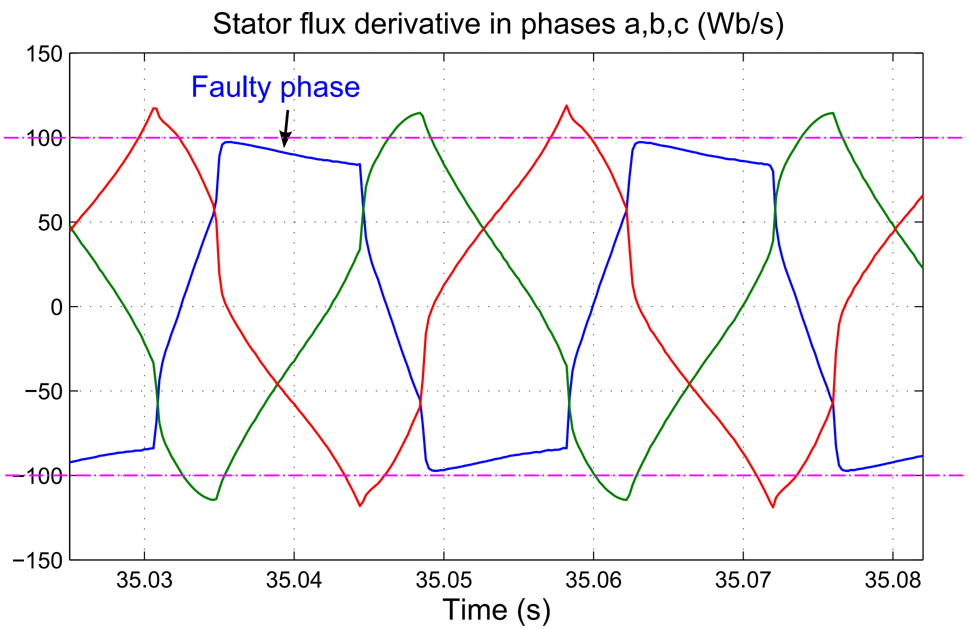

Experimental results

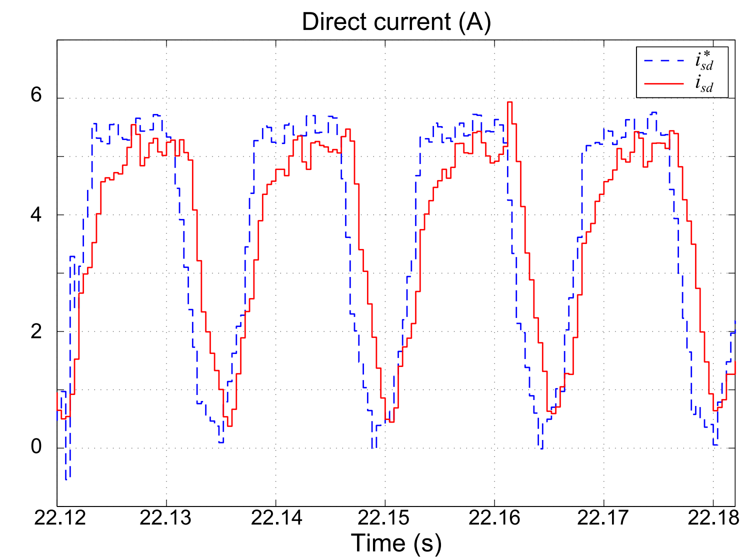

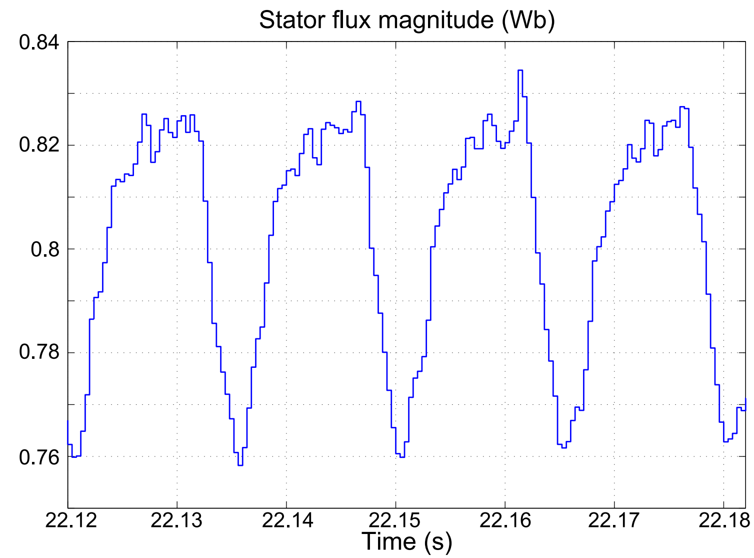

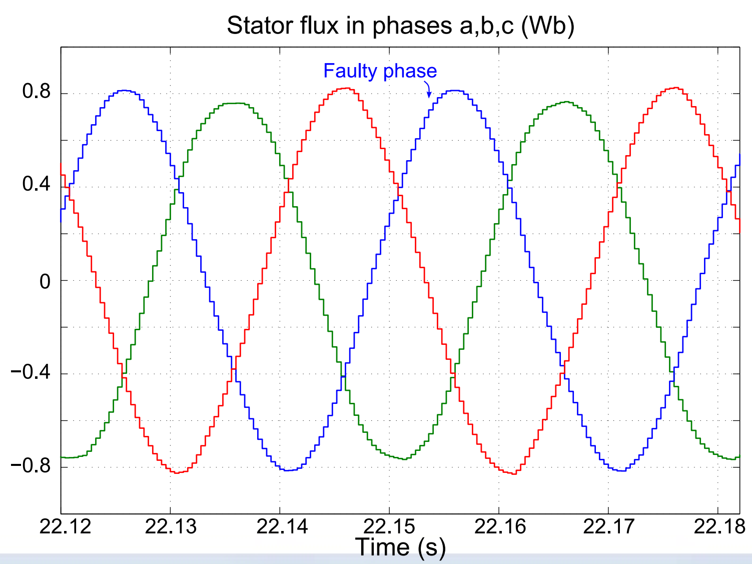

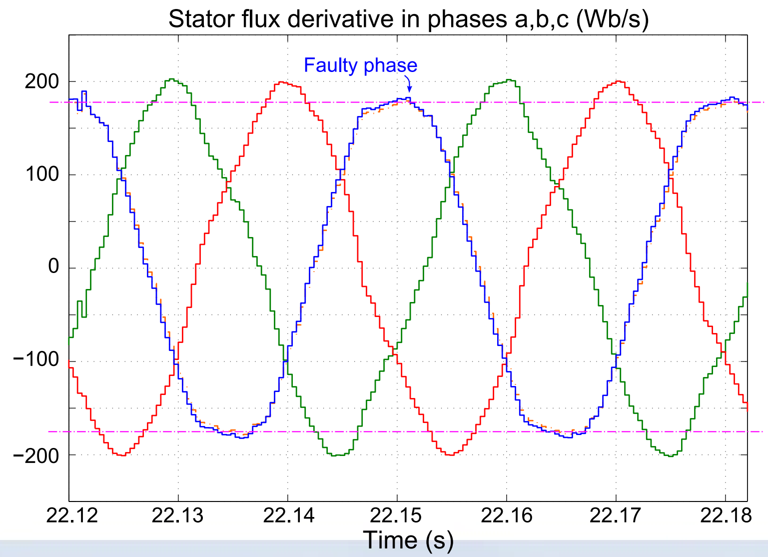

Experimental results

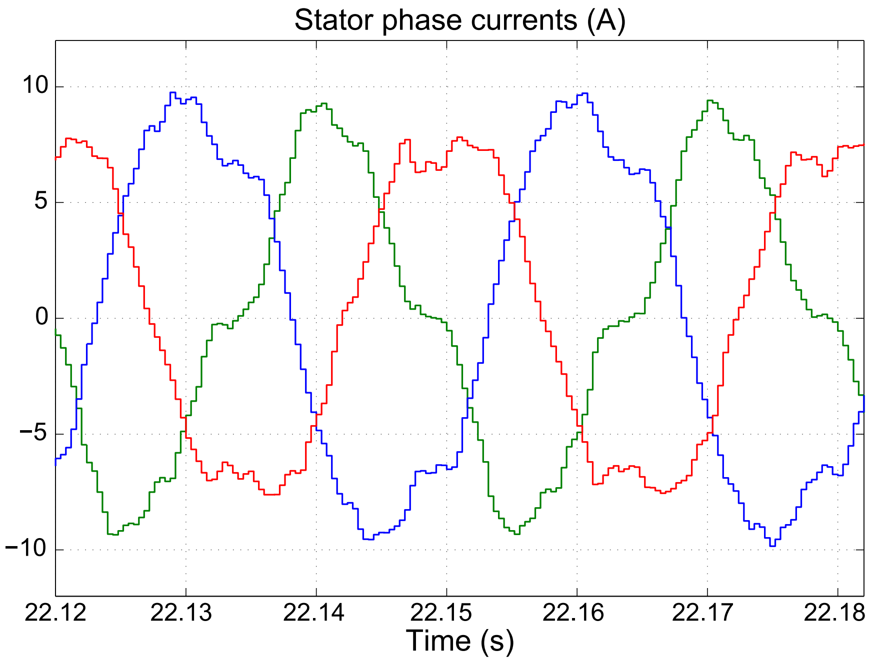

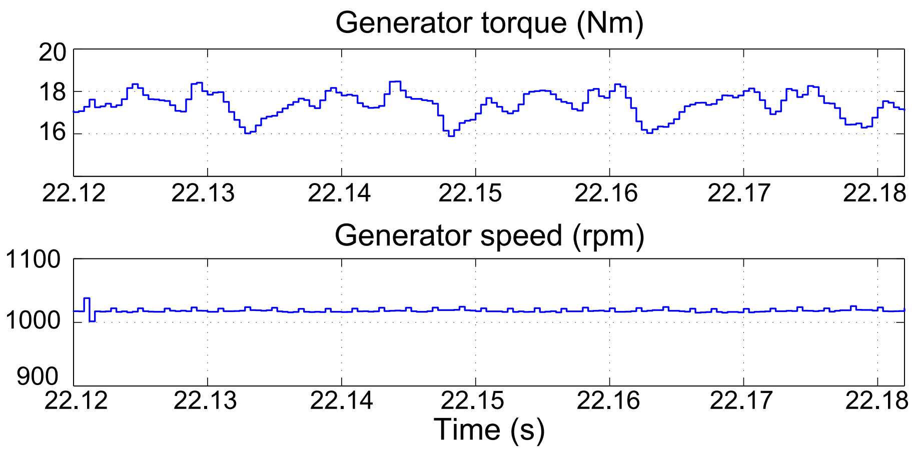

PMSG stator insulation FTC

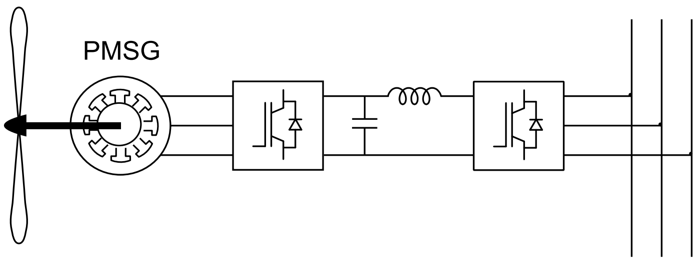

Description	Parameter	Value
Rated power	P_{gn}	2 MW
Rated frequency	f_n	12.64 Hz
Number of pole pairs	p	32
Stator resistance	R_s	0.01 Ω
Stator inductance in d-axis	L_{sd}	3 mH
Stator inductance in q-axis	L_{sq}	3 mH
Permanent magnets flux	ψ_r	12.9 Wb

WT operating area for K_{FTC} = 600 Wb/s

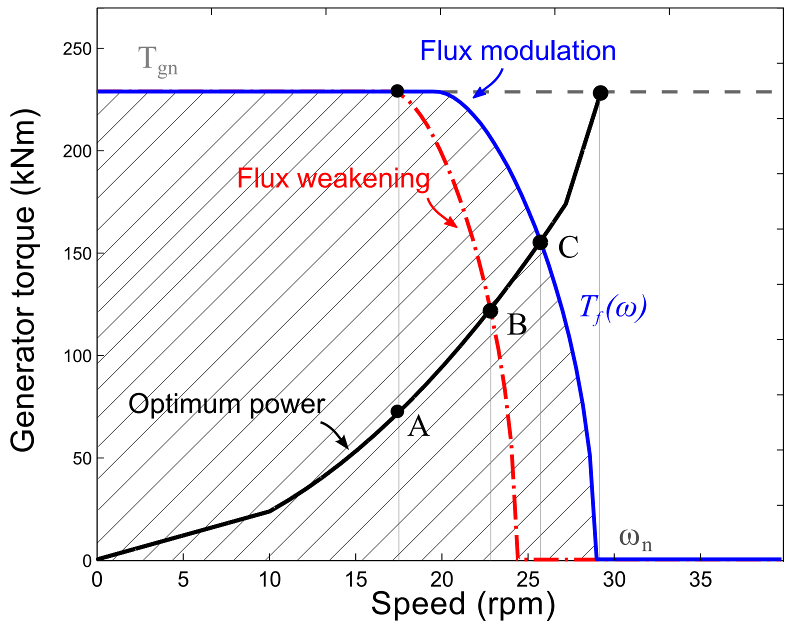

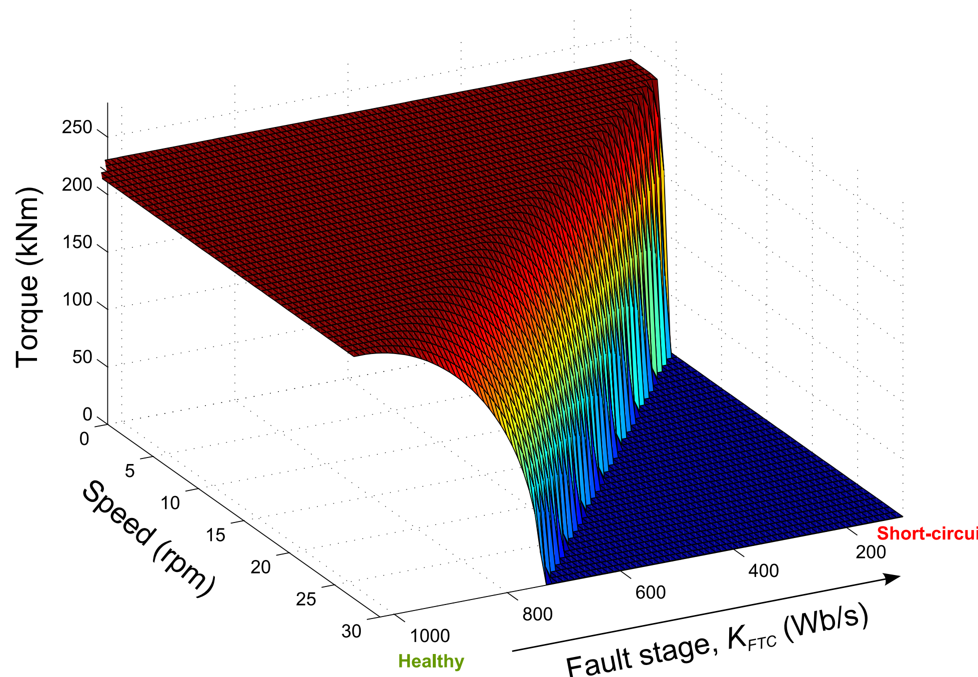

$$T_g = \frac{3}{2} p \psi_{pm} i_{sq} \quad \Rightarrow \quad T_g = \frac{3}{2} p \left[\psi_{pm} + \left(L_{sd} - L_{sq} \right) i_{sd} \right] i_{sq}$$

WRSG stator insulation FTC

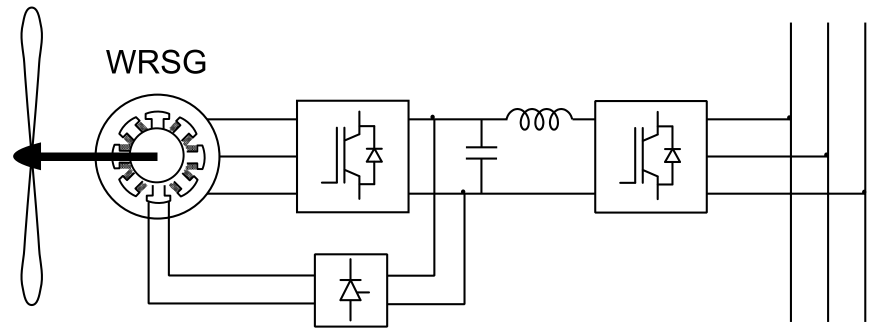

Rated power	P_{gn}	1800 kVA
Rated voltage	U_n	1250 V
Rated frequency	f_n	13.5 Hz
Number of pole pairs	p	30
Stator resistance	R_s	0.022 Ω
Stator inductance in d-axis	L_{sd}	12.18 mH
Stator inductance in q-axis	L_{sq}	8.53 mH
Stator mutual inductance	L_{md}	10.46 mH
Rotor inductance	L_f	12.65 mH
Rotor resistance	R_f	1.24 Ω
Rated excitation voltage	U_f	800 V

WT operating area for K_{FTC} = 600 Wb/s

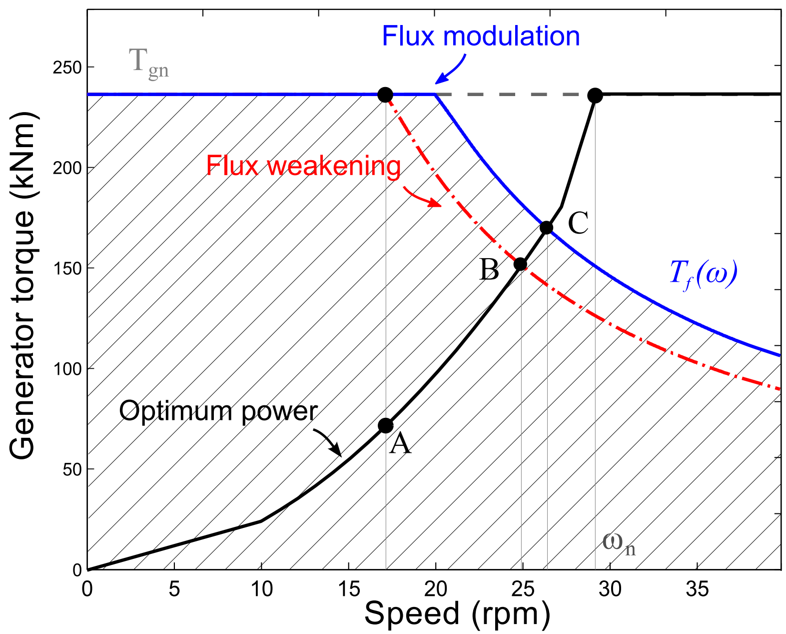

DFIG rotor insulation FTC

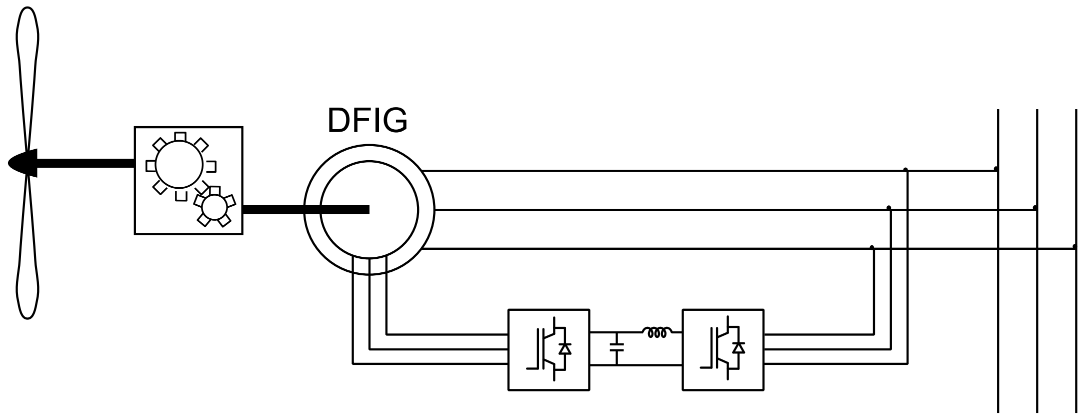

Description	Parameter	Value
Rated power	P_{gn}	1.5 MW
Rated frequency	f_n	50 Hz
Number of pole pairs	p	2
Rated rotor speed	n_n	1750 rpm
Rated slip	ω_{sln}	0.1667
Rated stator current	I_{sn}	1068.2 A (rms)
Rated rotor current	I_{rn}	1125.6 A (rms)
Rated stator phase voltage	U_{sn}	398.4 V (rms)
Rated rotor phase voltage	U_{rn}	67.97 V (rms)
Stator resistance	R_s	2.65 $m\Omega$
Rotor resistance	R_r	2.63 $m\Omega$
Stator inductance	L_s	5.6436 mH
Rotor inductance	L_r	5.6086 mH
Mutual inductance	L_m	5.4749 mH
Rated rotor flux	ψ_{rn}	1.9073 Wb

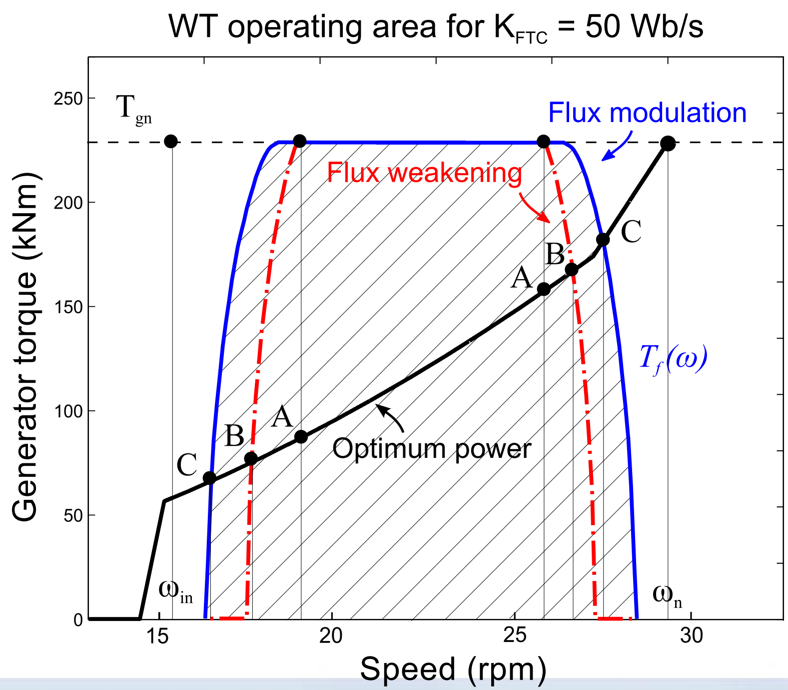

Unconstrained optimal control

$$\frac{i_{sd}(s)}{i_{sd}^{*}(s)} = \frac{1}{1+\tau \cdot s}$$

$$\frac{\psi_{rd}(s)}{i_{sd}(s)} = \frac{L_m}{1+T_r \cdot s}$$

$$\left.\right\} \quad \begin{aligned} x_{k+1} &= \mathbf{A}x_k + \mathbf{B}u_k \\ y_k &= \mathbf{C}x_k \end{aligned}$$

$$x = \begin{bmatrix} i_{sd} \\ \psi_{rd} \end{bmatrix}$$

$$u = i_{sd}^{*}$$

$$y = \psi_{sd} = L_l i_{sd} + \frac{L_m}{L_r}\psi_{rd}$$

Time-critical: $T_s = 200\mu s$

Cost function:

– $\psi_{sd}(t)$ tracks reference $\psi_{sd}^{*}(t)$

$$J = \left(\mathbf{C}^{*}X - \mathbf{R}\right)^T \mathbf{Q}\left(\mathbf{C}^{*}X - \mathbf{R}\right) = U^T HU + fU + g$$

minimise J → On-line control law:

$$H = \mathbf{B}^{*T}\mathbf{C}^{*T}\mathbf{Q}\mathbf{C}^{*}\mathbf{B}^{*}$$

$$f = 2\left(x_0^T \mathbf{A}^{*T}\mathbf{C}^{*T} - \mathbf{R}^T\right)\mathbf{Q}\mathbf{C}^{*}\mathbf{B}^{*}$$

$$\boxed{U = -\frac{1}{2}H^{-1}f^T}$$

Simulation results

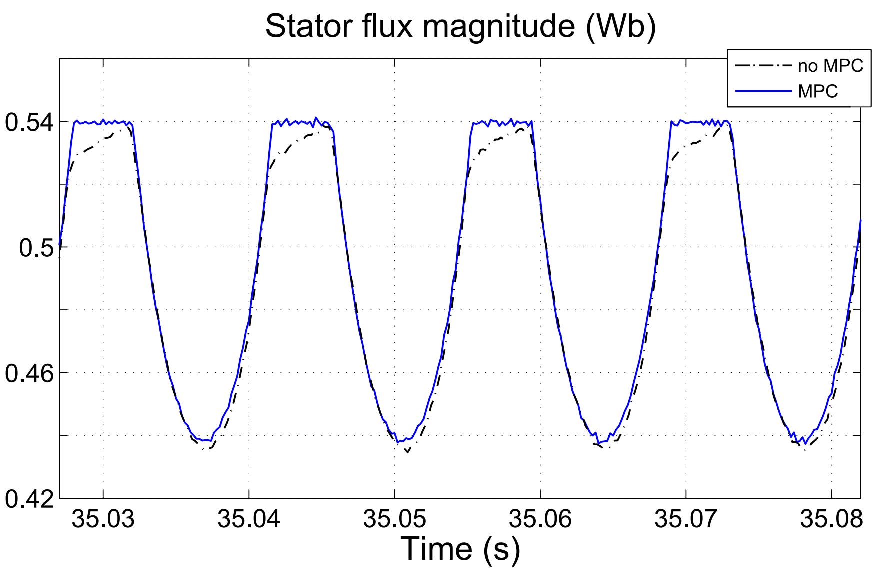

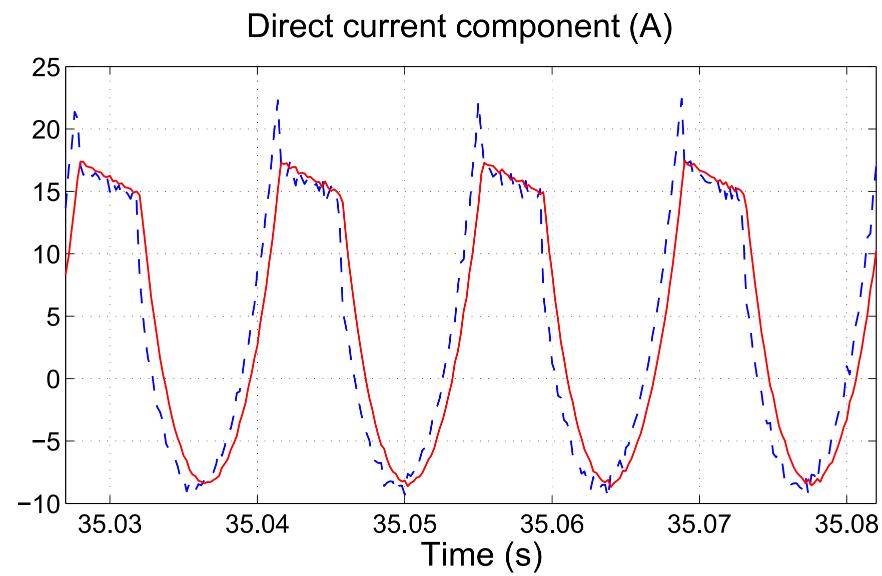

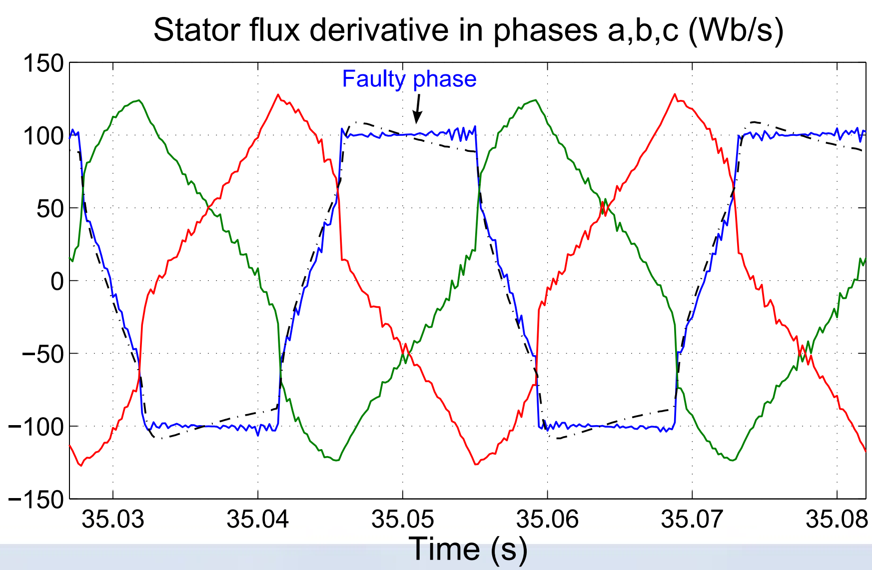

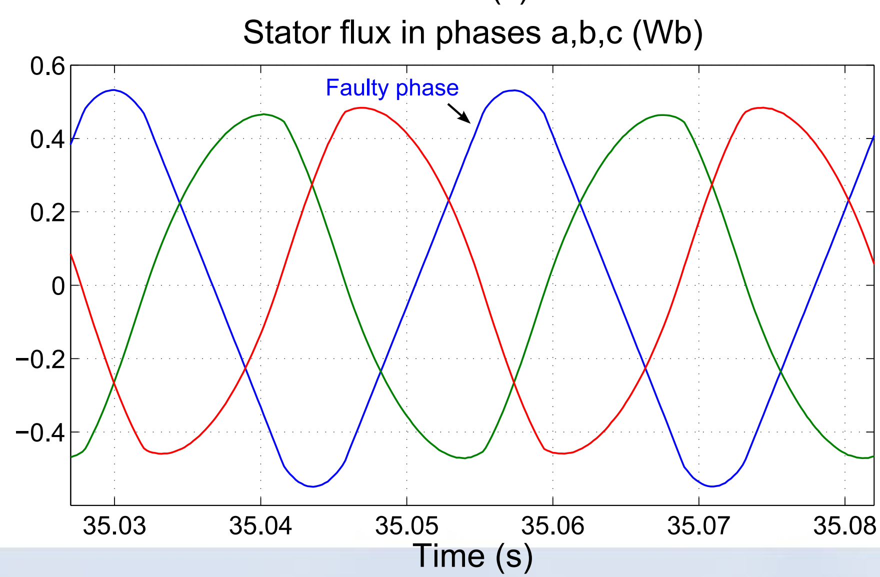

Simulation results – MPC

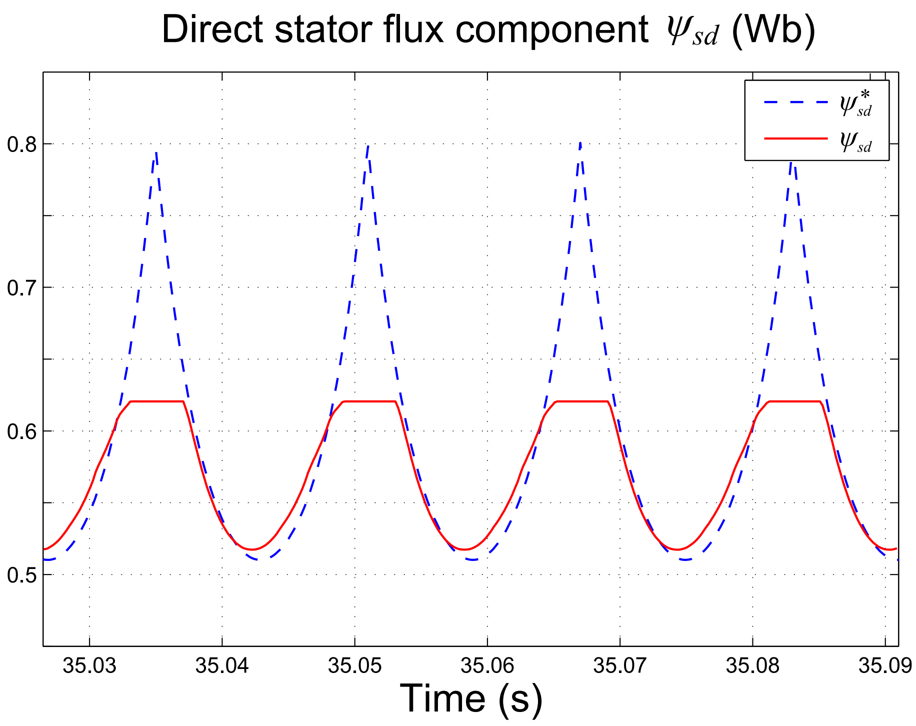

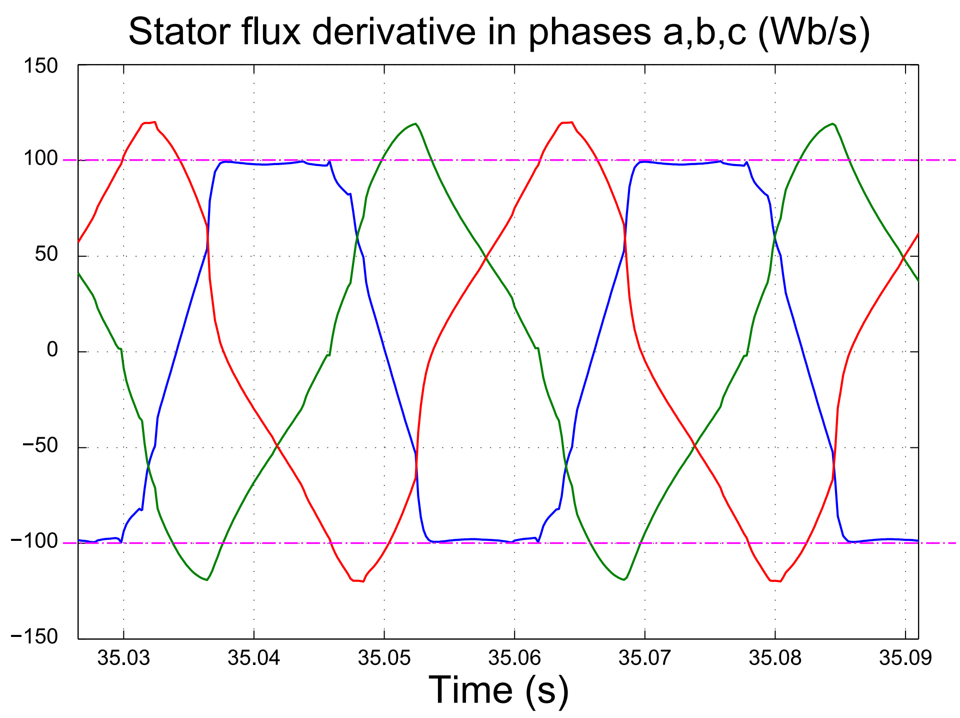

Utjecaj na sustav vjetroagregata

Structural loads

- Rotor cage defect fault-tolerant control

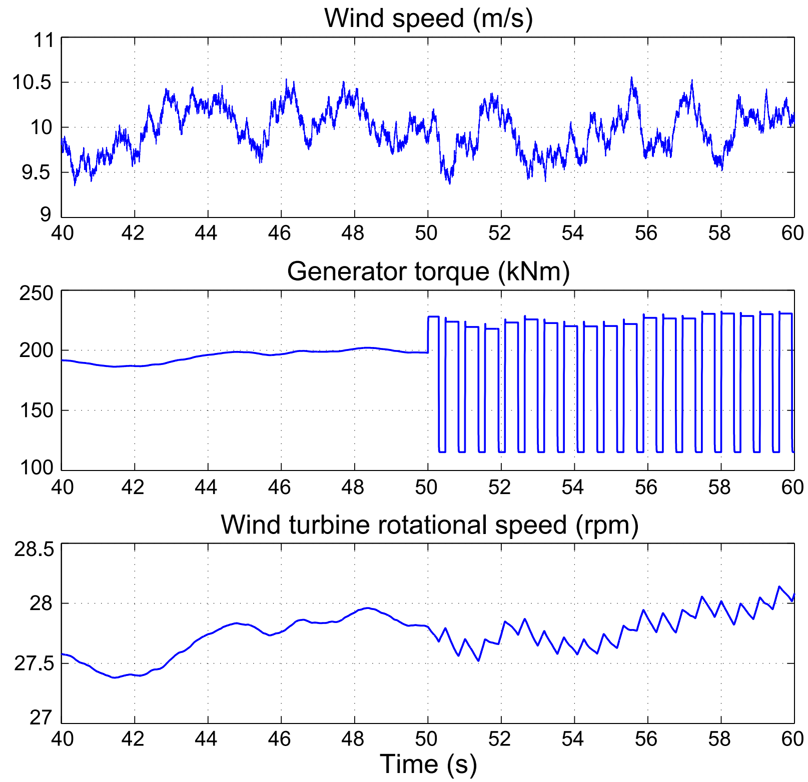

Structural loads

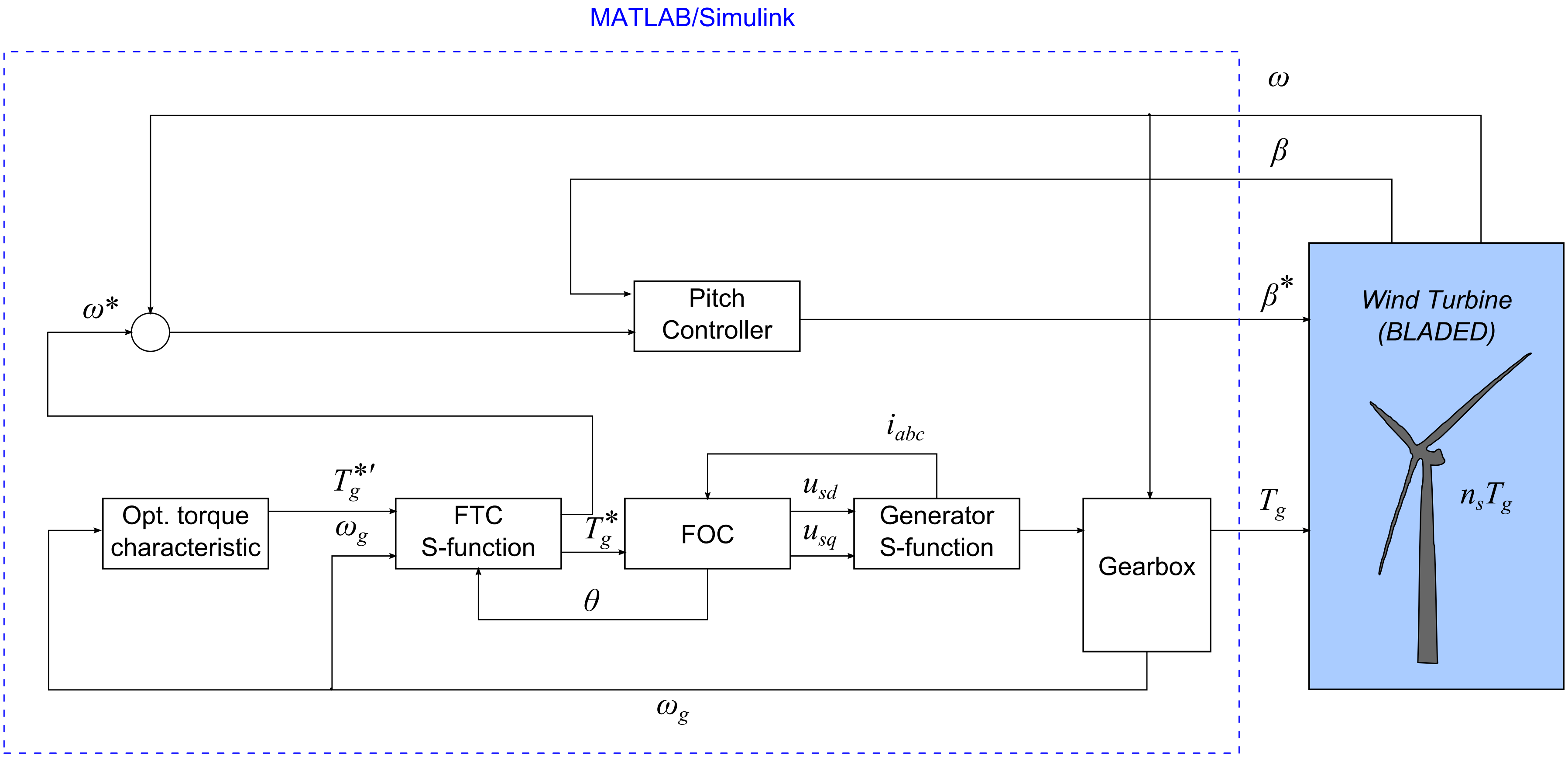

Structural loads in turbulent wind

Blade root

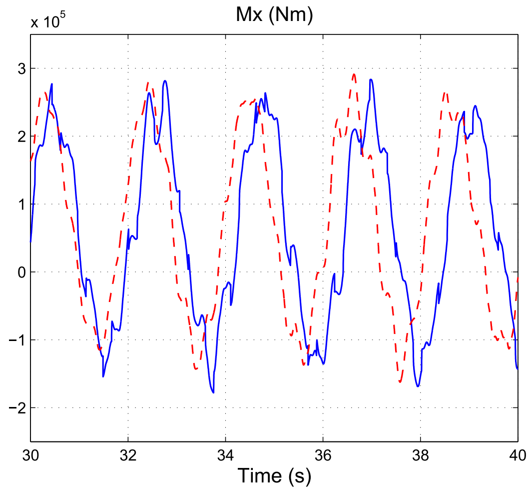

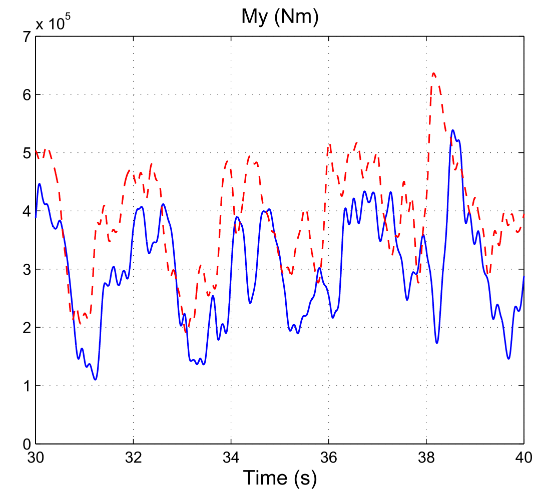

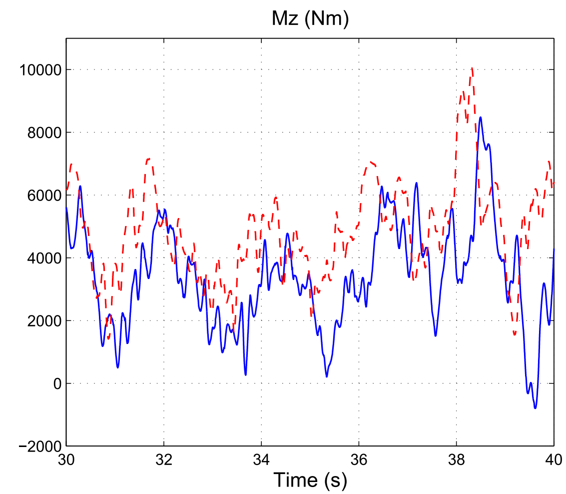

Blade root

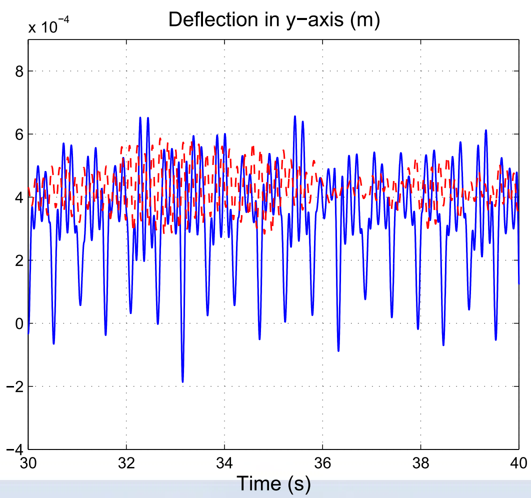

Tower tip

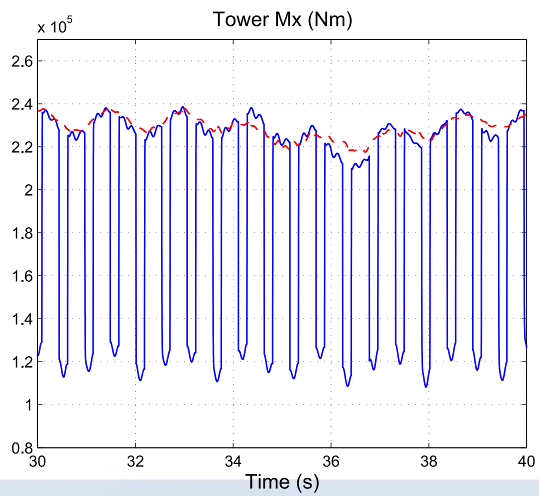

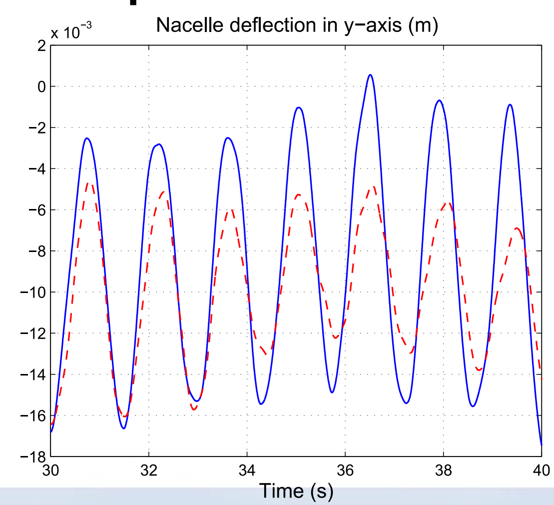

Structural loads in turbulent wind

Blade root

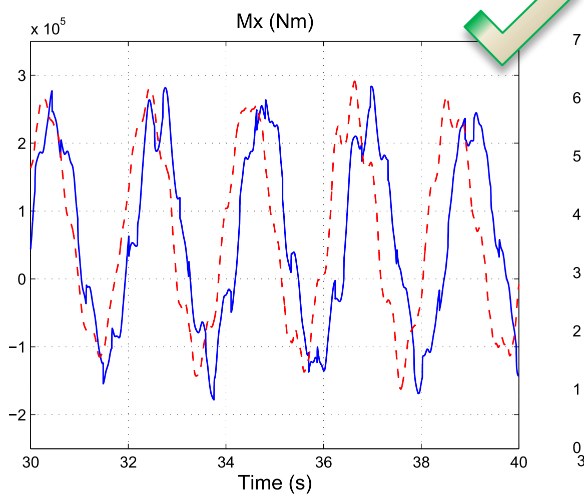

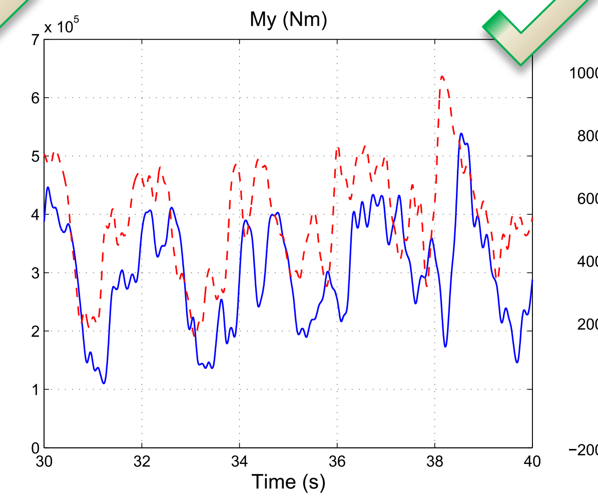

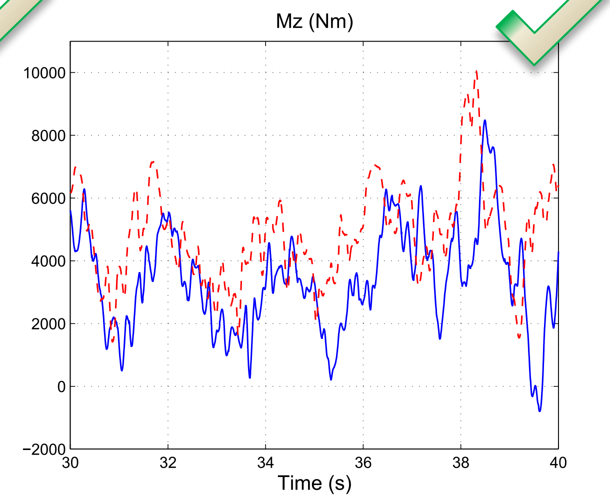

Blade root

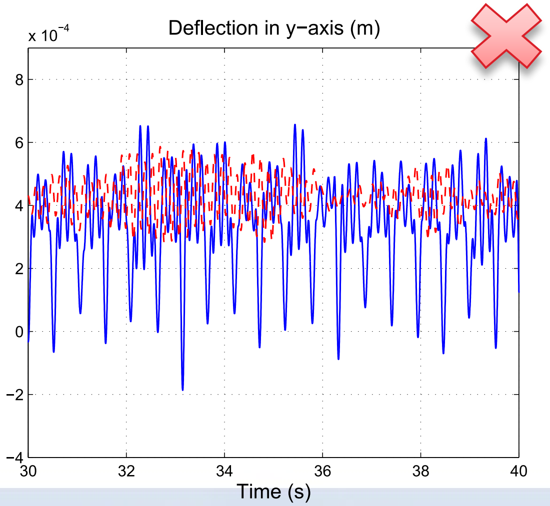

Tower tip

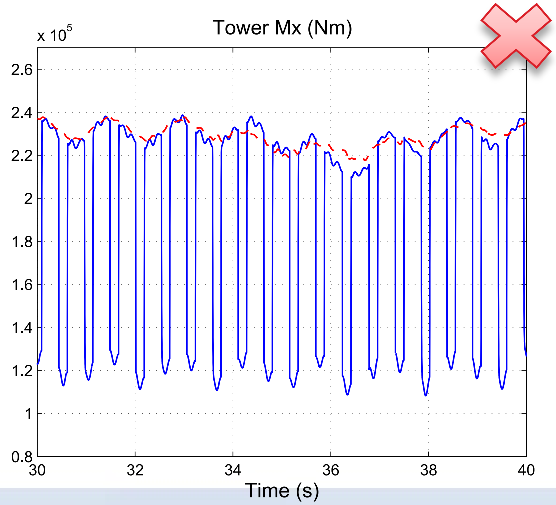

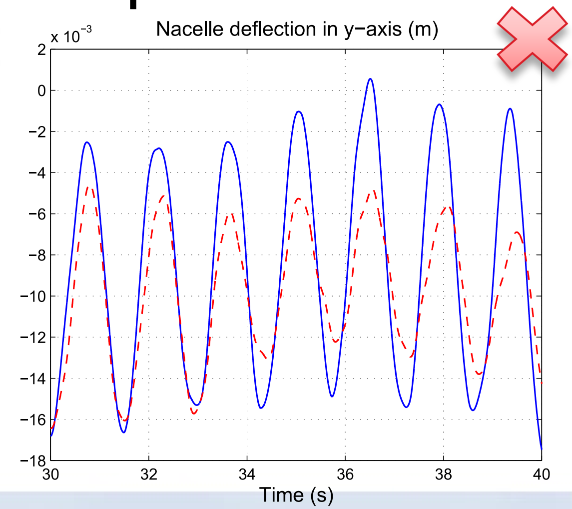

Power production quality

- Stator insulation fault-tolerant control

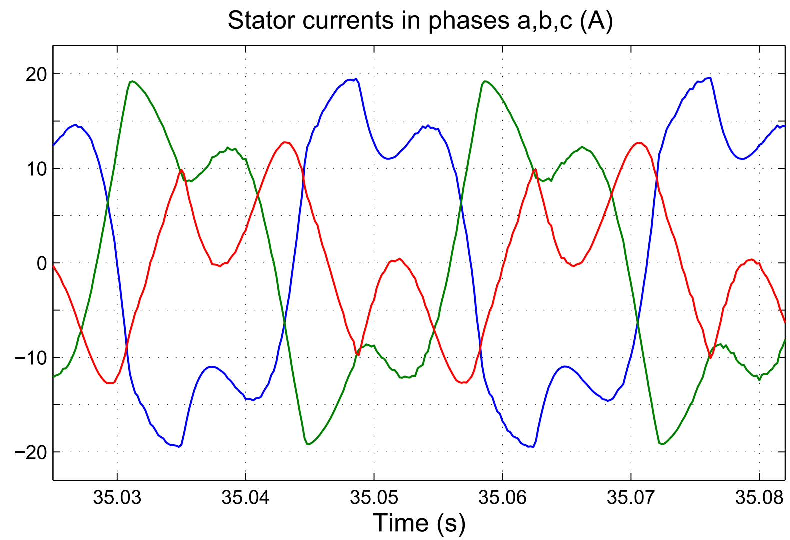

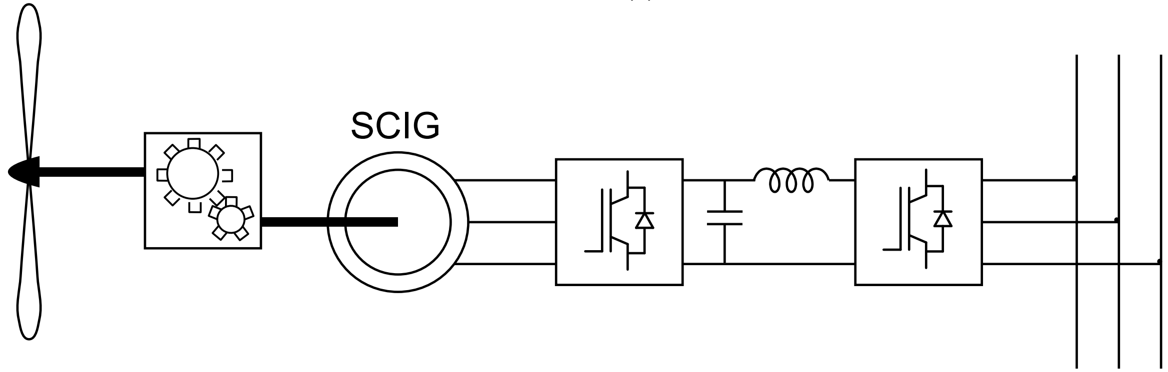

Power production quality

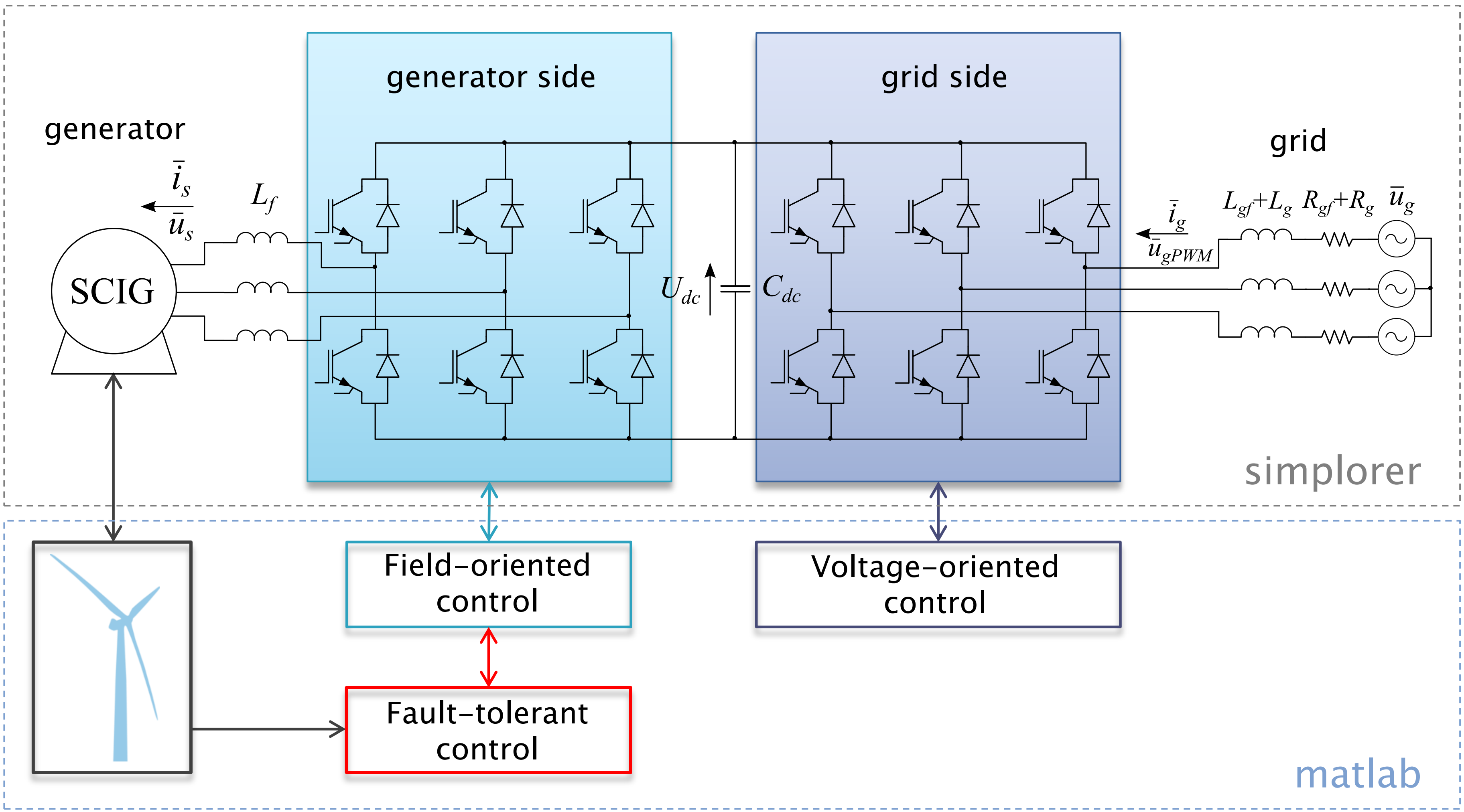

Power production quality

- THD increase from 2.51% to 2.95%

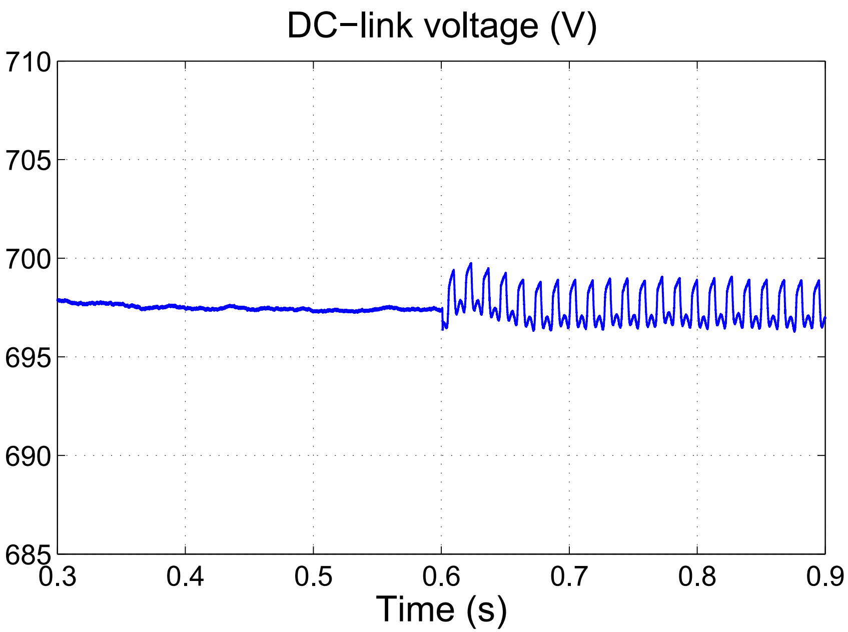

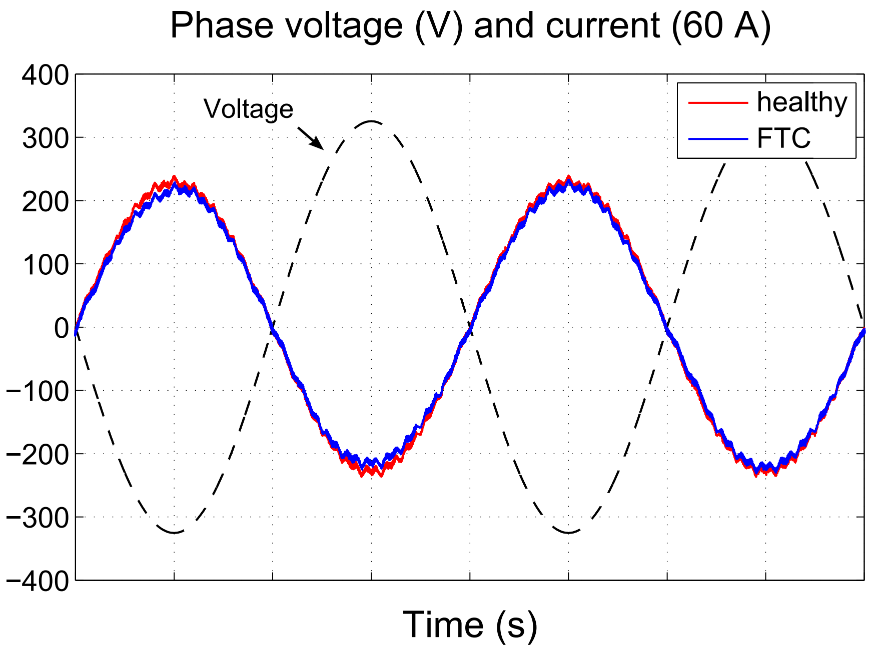

Smanjenje vibracija pri upravljanju momentom generatora

Anisotropic FOC

$$L_l = L_{offset} \quad \longrightarrow \quad \overline{L}_{l,t} = L_{offset} + L_{mod} \cdot e^{j2\gamma}$$

Anisotropic FOC

Location

$$L_l = L_{offset} \quad \longrightarrow \quad \bar{L}_{l,t} = L_{offset} + L_{mod} \cdot e^{j2\gamma}$$

Value

Anisotropic FOC

Location

$$L_l = L_{offset} \longrightarrow \overline{L}_{l,t} = L_{offset} + L_{mod} \cdot e^{j2\gamma}$$

Value

dq model:

$$L_{ld} = L_{offset} + L_{mod} \cdot \cos(2\gamma)$$

$$L_{lq} = L_{mod} \cdot \sin(2\gamma)$$

Anisotropic FOC

$$L_l = L_{offset} \longrightarrow \overline{L}_{l,t} = L_{offset} + L_{mod} \cdot e^{j2\gamma}$$

Location

Value

dq model:

$$L_{ld} = L_{offset} + L_{mod} \cdot \cos(2\gamma)$$

$$L_{lq} = L_{mod} \cdot \sin(2\gamma)$$

Leakage inductance in d-axis (mH)

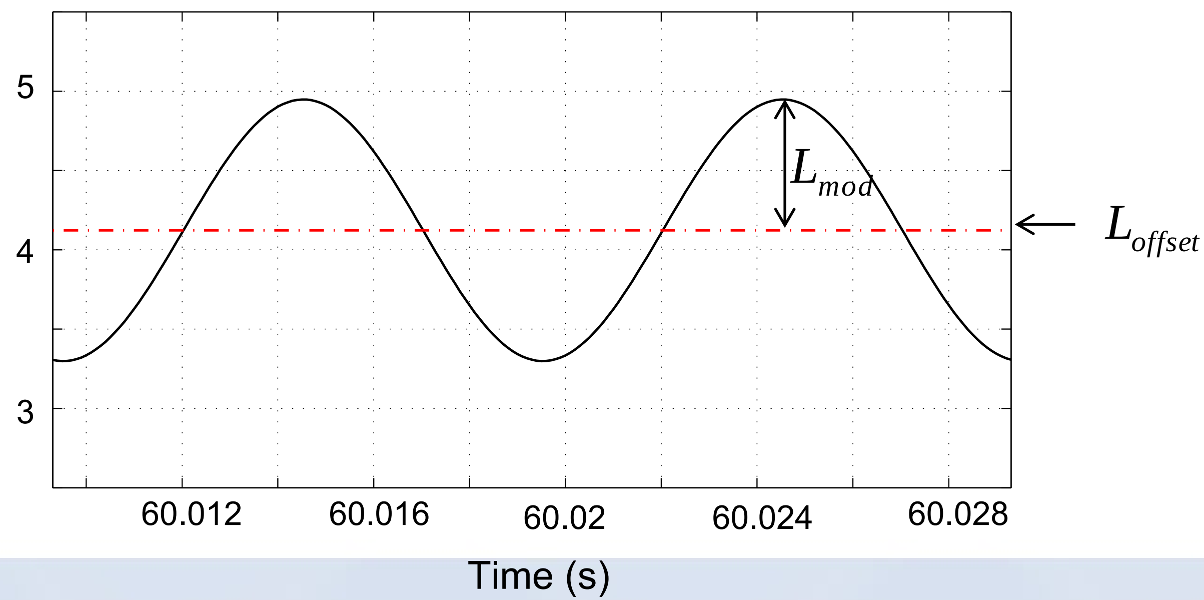

Total anisotropy

$$L_{ld} = L_l + L_{\text{mod},e} \cdot \cos(2\gamma_e) + L_{\text{mod},s} \cdot \cos(2\gamma_s)$$
$$+ L_{\text{mod},r} \cdot \cos(2\gamma_r) + L_{\text{mod},b} \cdot \cos(2\gamma_b)$$

$$L_{lq} = L_{\text{mod},e} \cdot \sin(2\gamma_e) + L_{\text{mod},s} \cdot \sin(2\gamma_s)$$
$$+ L_{\text{mod},r} \cdot \sin(2\gamma_r) + L_{\text{mod},b} \cdot \sin(2\gamma_b)$$

$$\gamma_e \longleftrightarrow \omega_e$$
$$\gamma_s \longleftrightarrow N_s\omega_e$$
$$\gamma_r \longleftrightarrow \omega_{sl}$$
$$\gamma_b \longleftrightarrow N_b\omega_{sl}$$

- Stator anisotropy:
  - Saturation saliency (blue)
  - Slots anisotropy (red)
- Rotor anisotropy:
  - Cage defects (orange)
  - Bars anisotropy (green)

Anisotropic FOC

- Model

$$u_{sd} + \Delta u_{sd} = k_a i_{sd} + L_a \frac{di_{sd}}{dt} \qquad k_a = R_s - \frac{L_a - L_s}{T_r}$$

$$u_{sq} + \Delta u_{sq} = R_s i_{sq} + L_a \frac{di_{sq}}{dt}$$

- Conventional model

$$\Delta u_{sd} = \frac{L_s - L_a}{T_r} i_{mr} + \omega_e L_a i_{sq}$$

$$\Delta u_{sq} = -\omega_e \left(L_s - L_a\right) i_{mr} - \omega_e L_a i_{sd}$$

$$L_a = L_l$$

Anisotropic FOC

- Model

$$u_{sd} + \Delta u_{sd} = k_a i_{sd} + L_a \frac{di_{sd}}{dt} \qquad k_a = R_s - \frac{L_a - L_s}{T_r}$$

$$u_{sq} + \Delta u_{sq} = R_s i_{sq} + L_a \frac{di_{sq}}{dt}$$

- Anisotropic model

$$L_a = L_{ld} + \frac{L_{lq}^2}{L_{ld}}$$

$$\Delta u_{sd} = \frac{L_{lq}}{L_{ld}} u_{sq} - \left(\frac{L_{lq}}{L_{ld}} R_s - \omega_e L_a \right) i_{sq} + \left(\frac{L_s - L_a}{T_r} - \omega_e \frac{L_{lq}}{L_{ld}} L_s \right) i_{mr}$$

$$\Delta u_{sd} = -\frac{L_{lq}}{L_{ld}} u_{sd} + \left(\frac{L_{lq}}{L_{ld}} R_s + \frac{L_{lq}}{L_{ld}} \frac{L_s}{T_r} - \omega_e L_a \right) i_{sd} - \left(\frac{L_{lq}}{L_{ld}} \frac{L_s}{T_r} + \omega_e \left(L_s - L_a \right) \right) i_{mr}$$

Simulation results

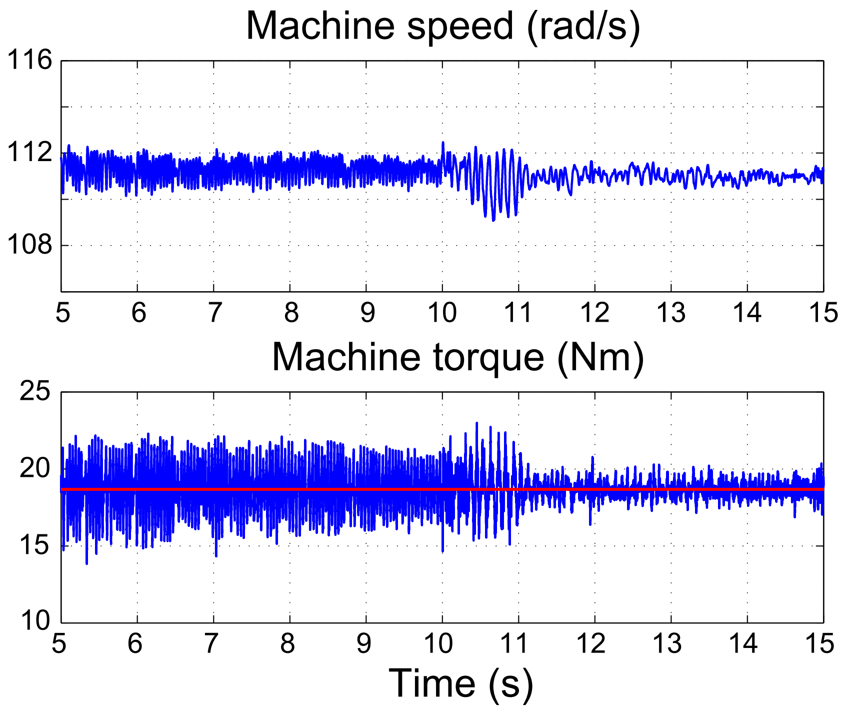

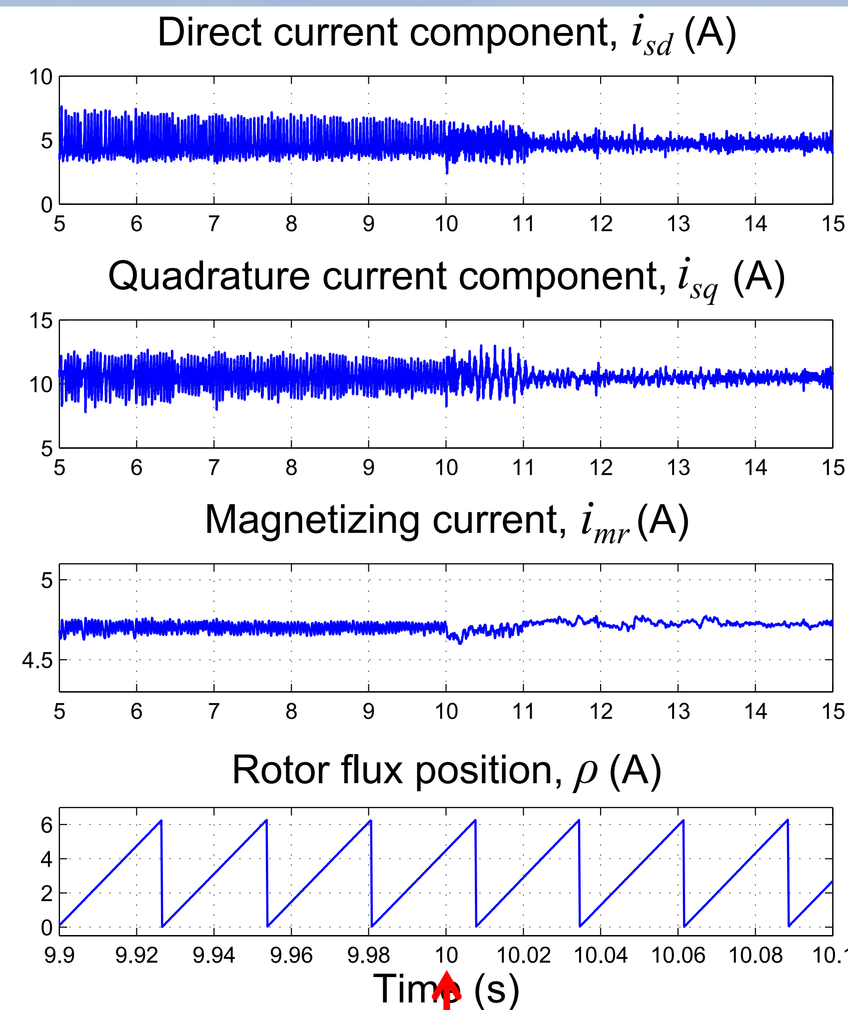

Estimation turned on at t=10 s

Damage equivalent loads

- Cyclic stress on the shaft → causes material fatigue
- MLife toolbox, developed by NREL

Constant load

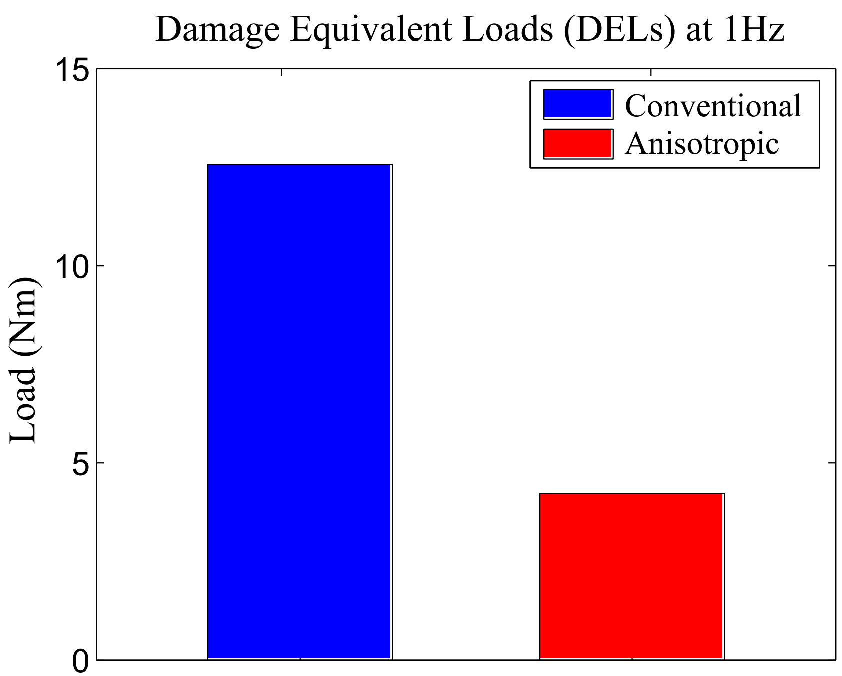

- 66% reduction

Dynamical load

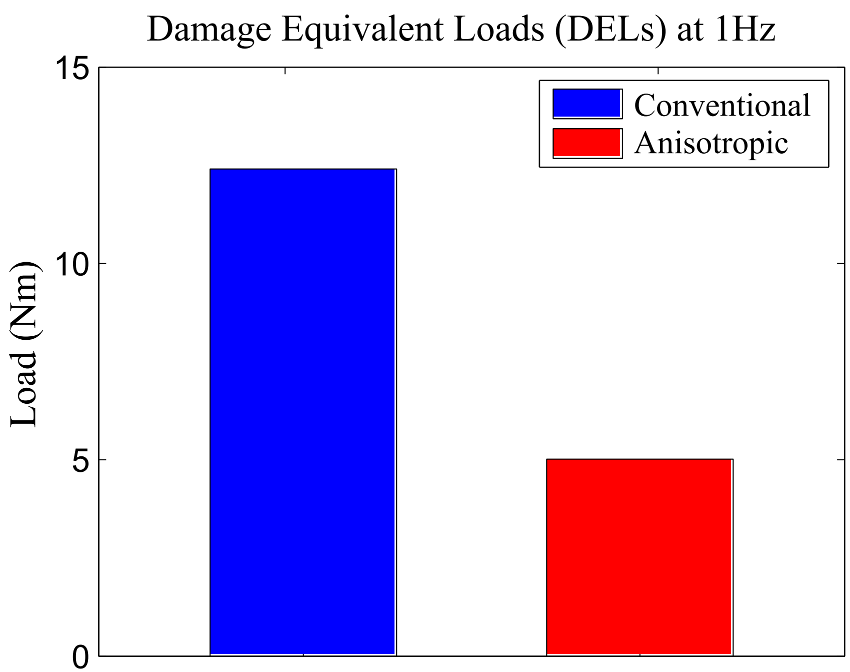

- 59% reduction

Zaključak

- Considered generator faults can be suppressed by proper manipulation of variables that cause rapid fault spreading
- The sooner the fault is detected, the more power is extracted with proposed methods
- Methods offer additional reliability centered maintenance possibilities
- Broad application in electrical drives

Zahvala

Projekte **CEEStructHealth** i **Will4Wind** sufinancira Europska unija kroz Europski fond za regionalni razvoj.

Dodatne informacije: http://act.rasip.fer.hr/

LARES Laboratorij za sustave obnovljivih izvora energije
vjetar sunce vodik

Ulaganje u budućnost!
STRUKTURNI I INVESTICIJSKI FONDOVI
KONKURENTNA HRVATSKA
FOND ZA ULAGANJE U ZNANOST I INOVACIJE
Ministarstvo znanosti, obrazovanja i sporta

Projekt je sufinancirala Europska unija iz Europskog fonda za regionalni razvoj

Hvala na pažnji!

http://act.rasip.fer.hr
vinko.lesic@fer.hr

Machine losses

- Sinusoidal current vs squared voltage increases iron losses by about 40%

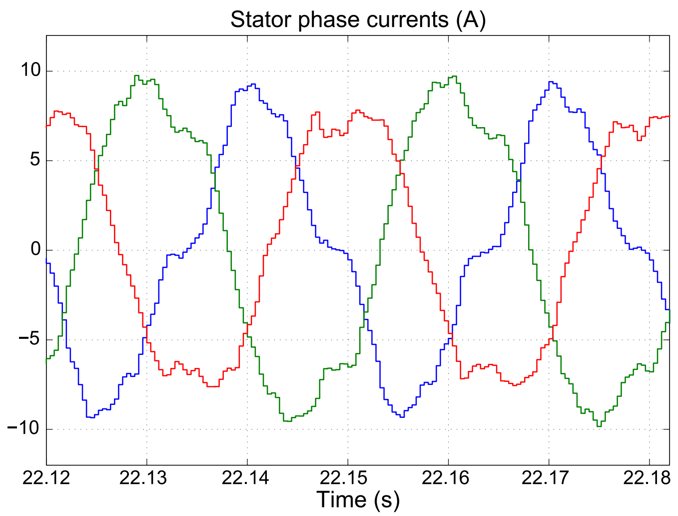

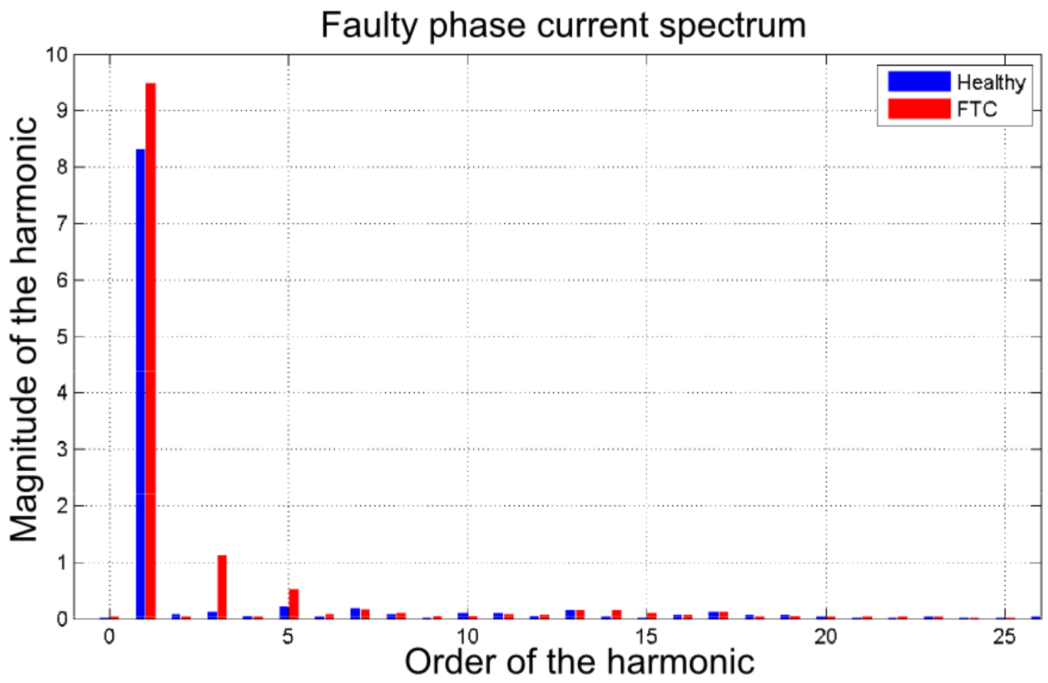

- Increase in 3rd harmonic

Wind farms in Croatia

Wind farm	Installed power (MW)	Region	Annual production (GWh)	Wind turbine models	Put in operation
VE Danilo	43	Šibensko-kninska županija	100	19 × Enercon E-82 – 2.3 MW	2014.
VE Vrataruša	42	Ličko-senjska županija	125	14 × Vestas V90 - 3 MW	2011.
VE Kamensko-Voštane	40	Splitsko-dalmatinska županija	114	14 × Siemens SWT-3.0-101 – 3 MW	2013.
VE Bruška (ZD2+ZD3)	36	Zadarska županija	122	16 × Siemens SWT-93 - 2,3 MW	2012.
VE Ponikve	34	Dubrovačko-neretvanska županija	100	16 x Enercon E-70 – 2,3 MW	2012.
VE Jelinak	30	Splitsko-dalmatinska županija	81	20 x Acciona AW-1500 – 1,5 MW	2013.
VE Pometeno Brdo	17.5	Splitsko-dalmatinska županija	30	15 × Končar KO-VA 57/1 – 1 MW +1 × Končar VA K80 – 2,5 MW	2012.
VE Trtar-Krtolin	11.2	Šibensko-kninska županija	28	14 × Enercon E-48 - 0,8 MW	2006.
VE Crno Brdo	10	Šibensko-kninska županija	27	7 × Leitwind LTW77 – 1,5 MW	2011.
VE Orlice	9.6	Šibensko-kninska županija	25	11 × Enercon (3 x E-48 – 0,8 MW + 8 × E-44 – 0,9 MW)	2009.
VE ZD 4 faza I	9.2	Zadarska županija	26	4 × Siemens SWT 93 – 2,3 MW	2013.
VE Velika Popina (ZD6)	9	Zadarska županija	26	4 × Siemens SWT 93 – 2,3 MW	2011.
VE Ravne	5.95	Zadarska županija	15	7 × Vestas V52 – 0,85 MW	2005.

Total 297.45 MW

DFIG	WRSG	SCIG	PMSG

Unconstrained optimal control

$$\frac{i_{sd}(s)}{i^*_{sd}(s)} = \frac{1}{1+\tau s}, \qquad x = \begin{bmatrix} i_{sd} \\ \psi_{rd} \end{bmatrix}, \quad u = i^*_{sd}.$$

$$\frac{\psi_{rd}(s)}{i_{sd}(s)} = \frac{L_m}{1+T_r s}.$$

$$\begin{aligned} x_{k+1} &= \mathbf{A}x_k + \mathbf{B}u_k, \\ y_k &= \mathbf{C}x_k, \end{aligned}$$

$$\mathbf{A} = \begin{bmatrix} 1-\frac{T_s}{\tau} & 0 \\ \frac{T_s}{T_r} & 1-\frac{T_s}{\tau} \end{bmatrix}, \quad \mathbf{B} = \begin{bmatrix} \frac{T_s}{\tau} \\ 0 \end{bmatrix},$$

$$\mathbf{C} = \begin{bmatrix} L_l & \frac{L_m}{L_r} \end{bmatrix},$$

$$\begin{aligned} \mathcal{X} &= \mathbf{A}^* x_0 + \mathbf{B}^* \mathcal{U}, \\ \mathcal{Y} &= \mathbf{C}^* \mathcal{X}, \end{aligned}$$

$$\mathcal{X} = \begin{bmatrix} x_0 \\ x_1 \\ \vdots \\ x_N \end{bmatrix}, \quad \mathcal{Y} = \begin{bmatrix} y_0 \\ y_1 \\ \vdots \\ y_N \end{bmatrix}, \quad \mathcal{U} = \begin{bmatrix} u_0 \\ u_1 \\ \vdots \\ u_{N-1} \end{bmatrix},$$

$$\mathbf{A}^* = \begin{bmatrix} \mathbf{I} \\ \mathbf{A} \\ \mathbf{A}^2 \\ \vdots \\ \mathbf{A}^N \end{bmatrix}, \quad \mathbf{B}^* = \begin{bmatrix} 0 & \dots & \dots & 0 \\ \mathbf{B} & \dots & \dots & 0 \\ \mathbf{AB} & \mathbf{B} & \dots & 0 \\ \vdots & \ddots & \ddots & \vdots \\ \mathbf{A}^{N-1}\mathbf{B} & \dots & \dots & \mathbf{B} \end{bmatrix},$$

$$\mathbf{C}^* = \begin{bmatrix} \mathbf{C} & 0 & \dots & 0 \\ 0 & \mathbf{C} & \dots & 0 \\ \vdots & \ddots & \ddots & \vdots \\ 0 & 0 & \dots & \mathbf{C} \end{bmatrix}. \qquad (25)$$

$$J = \left(\mathbf{C}^* X - \mathbf{R}\right)^T \mathbf{Q} \left(\mathbf{C}^* X - \mathbf{R}\right) = U^T H U + fU + g \qquad U = -\frac{1}{2} H^{-1} f^T$$

$$\begin{aligned} \mathcal{H} &= \mathbf{B}^{*\top}\mathbf{C}^{*\top}\mathbf{Q}\mathbf{C}^*\mathbf{B}^*, \\ f &= 2x_0^\top \mathbf{A}^{*\top}\mathbf{C}^{*\top}\mathbf{Q}\mathbf{C}^*\mathbf{B}^* - 2\mathbf{R}^\top\mathbf{Q}\mathbf{C}^*\mathbf{B}^*, \\ g &= x_0^\top \mathbf{A}^{*\top}\mathbf{C}^{*\top}\mathbf{Q}\mathbf{C}^*\mathbf{A}^* x_0 - 2\mathbf{R}^\top\mathbf{Q}\mathbf{C}^*\mathbf{A}^* x_0 + \mathbf{R}^\top\mathbf{Q}\mathbf{R}. \end{aligned}$$

Inverse current flow

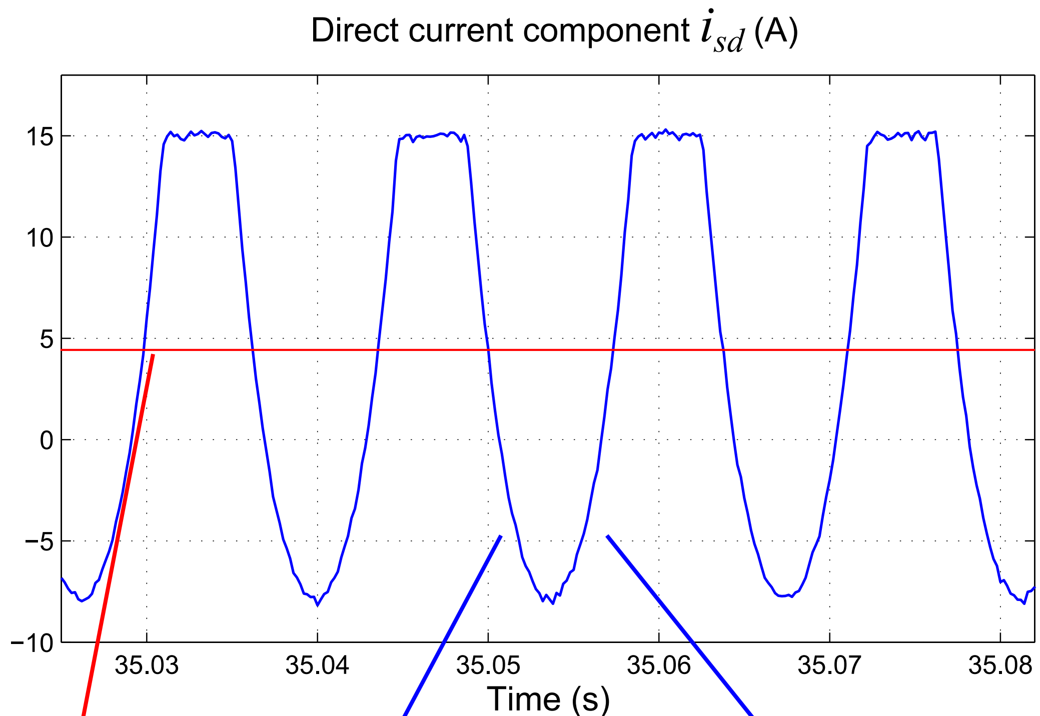

$$i_d^+ = I^+ \cos\delta^+ + I^- \cos\delta^- \cos 2\omega t + I^- \sin\delta^- \sin 2\omega t$$

DC component AC component

R. Teodorescu, M. Liserre, P. Rodriguez, “Grid converters for photovoltaic and wind power systems”